The Influence of Ca^{2+} Buffers on Free $[Ca^{2+}]$ Fluctuations and the Effective Volume of Ca^{2+} Microdomains

Seth H. Weinberg and Gregory D. Smith*
Department of Applied Science, The College of William & Mary, Williamsburg, Virginia

ABSTRACT Intracellular calcium (Ca^{2+}) plays a significant role in many cell signaling pathways, some of which are localized to spatially restricted microdomains. Ca^{2+} binding proteins (Ca^{2+} buffers) play an important role in regulating Ca^{2+} concentration ($[Ca^{2+}]$). Buffers typically slow $[Ca^{2+}]$ temporal dynamics and increase the effective volume of Ca^{2+} domains. Because fluctuations in $[Ca^{2+}]$ decrease in proportion to the square-root of a domain's physical volume, one might conjecture that buffers decrease $[Ca^{2+}]$ fluctuations and, consequently, mitigate the significance of small domain volume concerning Ca^{2+} signaling. We test this hypothesis through mathematical and computational analysis of idealized buffer-containing domains and their stochastic dynamics during free Ca^{2+} influx with passive exchange of both Ca^{2+} and buffer with bulk concentrations. We derive Langevin equations for the fluctuating dynamics of Ca^{2+} and buffer and use these stochastic differential equations to determine the magnitude of $[Ca^{2+}]$ fluctuations for different buffer parameters (e.g., dissociation constant and concentration). In marked contrast to expectations based on a naive application of the principle of effective volume as employed in deterministic models of Ca^{2+} signaling, we find that mobile and rapid buffers typically increase the magnitude of domain $[Ca^{2+}]$ fluctuations during periods of Ca^{2+} influx, whereas stationary (immobile) Ca^{2+} buffers do not. Also contrary to expectations, we find that in the absence of Ca^{2+} influx, buffers influence the temporal characteristics, but not the magnitude, of $[Ca^{2+}]$ fluctuations. We derive an analytical formula describing the influence of rapid Ca^{2+} buffers on $[Ca^{2+}]$ fluctuations and, importantly, identify the stochastic analog of (deterministic) effective domain volume. Our results demonstrate that Ca^{2+} buffers alter the dynamics of $[Ca^{2+}]$ fluctuations in a nonintuitive manner. The finding that Ca^{2+} buffers do not suppress intrinsic domain $[Ca^{2+}]$ fluctuations raises the intriguing question of whether or not $[Ca^{2+}]$ fluctuations are a physiologically significant aspect of local Ca^{2+} signaling.

INTRODUCTION

The regulation of intracellular calcium (Ca^{2+}) concentration ($[Ca^{2+}]$) is a fundamental aspect of many cell signaling pathways (1). In many types of cells, spatially localized Ca^{2+} signals known as Ca^{2+} micro- or nanodomains regulate specific cellular processes in different subcellular regions. Significant examples include pre- and postsynaptic signaling in neuronal dendrites (2–4), contraction regulation in cardiac dyadic subspaces (3,5–7), localized control of mitochondria (8–10), and nuclear gene transcription (4,8), and localized mechanical and olfactory sensing in primary cilia (11–13).

Ca^{2+} buffers play an important role in modulating spatially localizing Ca^{2+} signals. The term "Ca^{2+} buffers" is generic and includes endogenous binding proteins, exogenous Ca^{2+} chelators (e.g., EGTA and BAPTA), indicator dyes (e.g., Fluo-4 and Rhod-2), and other nonspecific Ca^{2+} binding molecules (e.g., membrane phospholipids). In addition to regulating the levels of free Ca^{2+} in the cytoplasm, Ca^{2+} buffers influence the spatiotemporal dynamics of Ca^{2+} signaling. Because Ca^{2+} buffer binding rates, affinities, and diffusivities can range over several orders of magnitude (14), it is important to understand the influence of these parameters on Ca^{2+}-dependent signaling. Using deterministic formulations for Ca^{2+} and buffer dynamics, investigators have derived analytical results pertaining to the influence of rapid mobile and immobile buffers on Ca^{2+} signaling, demonstrating that buffers can greatly alter the $[Ca^{2+}]$ profile in the proximity of Ca^{2+} channels (15–19). Immobile buffers have been shown to reduce the effective diffusivity of Ca^{2+}, whereas mobile buffers can facilitate diffusion near an open Ca^{2+} channel and produce steep $[Ca^{2+}]$ gradients (20). Experimental and simulation studies have shown that the decay of residual Ca^{2+} after Ca^{2+} channel closure can be longer for rapid buffers than slow buffers (21,22). The influence of buffers on Ca^{2+} signaling can be counterintuitive, because it depends subtly on binding rate kinetics and competition between Ca^{2+}-binding sites. For example, analytical results have shown that increased buffer diffusivity may increase or decrease the speed of a propagating Ca^{2+} wave, depending on the excitability of Ca^{2+} dynamics and buffer properties (23).

Assuming a rapidly equilibrating bimolecular association reaction between Ca^{2+} and buffer (B),

$$Ca^{2+} + B \underset{k_-}{\overset{k_+}{\rightleftharpoons}} CaB, \tag{1}$$

the time evolution of $[Ca^{2+}]$, denoted by c below, can be described by the ordinary differential equation (ODE) (24)

$$\Omega \dot{c} = \beta J, \tag{2}$$

where the dot indicates a time derivative, Ω is the compartmental volume, $J = J_{in} - J_{out}$ is the net flux of

Submitted December 12, 2013, and accepted for publication April 30, 2014.
*Correspondence: greg@wm.edu
Editor: James Sneyd.

0006-3495/14/06/2693/17 $2.00
http://dx.doi.org/10.1016/j.bpj.2014.04.045

Ca^{2+} molecules into the compartment, and the buffering factor β is the differential fraction of free-to-total Ca^{2+} that takes values between 0 and 1,

$$\beta = \frac{1}{1+w}, \text{ and}$$
$$w = \frac{b_T \kappa}{(c+\kappa)^2}. \quad (3)$$

In this expression, total buffer concentration $b_T = b + cb$ is the sum of free and Ca^{2+}-bound buffer concentration, b and cb, respectively; $\kappa = k_-/k_+$ is the dissociation constant for Ca^{2+}; and the ratio $w = b_T\kappa/(c+\kappa)^2$ is the buffering capacity, i.e., the differential fraction of bound-to-free Ca^{2+}. Concentration balance equations such as Eq. 2 are often written in the form

$$\Omega_{\text{eff}}\dot{c} = J, \quad (4)$$

where the effective volume Ω_{eff} is defined as $\Omega_{\text{eff}} = \Omega/\beta \geq \Omega$.

It is well known that the number of molecules in biochemical reaction networks randomly fluctuate, and the resulting concentration fluctuations for each chemical species are larger amplitude when the system size is small (25,26). For a sufficiently large system, i.e., large volume and number of molecules, concentration fluctuations become negligible and deterministic modeling is appropriate (26). However, in physiological settings of local Ca^{2+} signaling, i.e., Ca^{2+} microdomains, the system size is often small and concentration fluctuations may be significant. Intracellular $[Ca^{2+}]$ is very low in resting cells, typically 100 nM, and the volume of Ca^{2+} microdomains or subspaces are ~10^{-17}–10^{-15} liters, values that correspond to 0.6–60 Ca^{2+} ions at rest. A large amount of prior work has focused on the influence of stochastic gating of Ca^{2+}-regulated Ca^{2+} channels on $[Ca^{2+}]$ (19,27–32), but only a few have considered the role of concentration fluctuations associated with the small number of Ca^{2+} ions typically present in domains (30,33,34). The relative size of $[Ca^{2+}]$ fluctuations can be characterized by their coefficient of variation (c_v), defined as the standard deviation of $[Ca^{2+}]$ divided by the mean $[Ca^{2+}]$. In a spatially restricted domain and in the absence of Ca^{2+} buffers, the relative size of $[Ca^{2+}]$ fluctuations is given by (35)

$$c_v^0 = \frac{1}{\sqrt{c_{ss}\Omega}}, \quad (5)$$

where c_{ss} is the steady-state $[Ca^{2+}]$ and Ω is the physical volume of the domain (the superscripted 0 indicates no buffers). Because $c_{ss}\Omega$ is the number of Ca^{2+} ions in the domain, this expression is consistent with the influence of system size on molecular fluctuations well known in statistical physics (26). For the small volume domains mentioned above, this c_v^0 is in the range of 1.3–0.13. Our prior work suggests that fluctuations in $[Ca^{2+}]$ of this magnitude could significantly influence the gating of Ca^{2+}-regulated Ca^{2+} channels in Ca^{2+} microdomains, such as dyadic subspaces or dendritic spines (35).

Although prior work makes it clear that $[Ca^{2+}]$ fluctuations are a nonnegligible aspect of Ca^{2+} signaling, the influence of Ca^{2+} buffers on the dynamics of $[Ca^{2+}]$ fluctuations has not previously been studied. Based on the notion of effective volume, one might conjecture that buffers decrease $[Ca^{2+}]$ fluctuations and, consequently, mitigate the significance of small domain volume vis-a-vis downstream Ca^{2+} signaling (e.g., Ca^{2+}-triggered events). Do Ca^{2+} buffers influence $[Ca^{2+}]$ fluctuations? If so, how do these fluctuations depend on Ca^{2+} buffer properties such as dissociation constant and total concentration (Ca^{2+} free plus bound)? To answer these questions, we develop and analyze a minimal stochastic model that includes Ca^{2+} and buffer in a domain of small volume.

Our analysis focuses on Ca^{2+} microdomains that arise from Ca^{2+} influx into a spatially restricted subcellular compartment that may contain Ca^{2+} buffers, e.g., a dendritic spine or cardiac dyadic subspace (Fig. 1, *A* and *B*). The theory is most directly applicable to Ca^{2+} signaling complexes with membrane configurations or other obstructions to diffusion (e.g., molecular crowding) resulting in spatially confined Ca^{2+} signaling, for example, the primary cilium (Fig. 1 *C*), mitochondria-endoplasmic reticulum (ER) junctions, and presynaptic boutons (2–13). Free Ca^{2+} and buffer (Ca^{2+}-bound and -free) may exchange between domain and bulk via diffusion represented as a first-order reaction (Fig. 1 *D*). We specify the volume but not the detailed geometry of the spatially confined region that delimits the domain. Spatial gradients between domain and bulk are minimally represented in the model, but the microdomain itself is treated as a well-stirred compartment. The compartmental model formulation is most applicable and relevant to microdomains for which the time constant for domain escape is longer than the characteristic time for diffusion across the domain (36).

For clarity and readability, we first present the stochastic model representing $[Ca^{2+}]$ fluctuations in a microdomain with no Ca^{2+} buffer. This preliminary calculation illustrates our approach and provides a reference point in our interpretation of results that include influx and efflux of both Ca^{2+} and buffer. We perform parameter studies to determine how Ca^{2+} buffers influence the size of $[Ca^{2+}]$ fluctuations, derive the fluctuating rapid buffer approximation to the dynamics of domain $[Ca^{2+}]$ fluctuations, and illustrate how the influence of buffers on the effective system size and the time course of $[Ca^{2+}]$ fluctuations depend on buffer parameters. We conclude with a discussion of our findings.

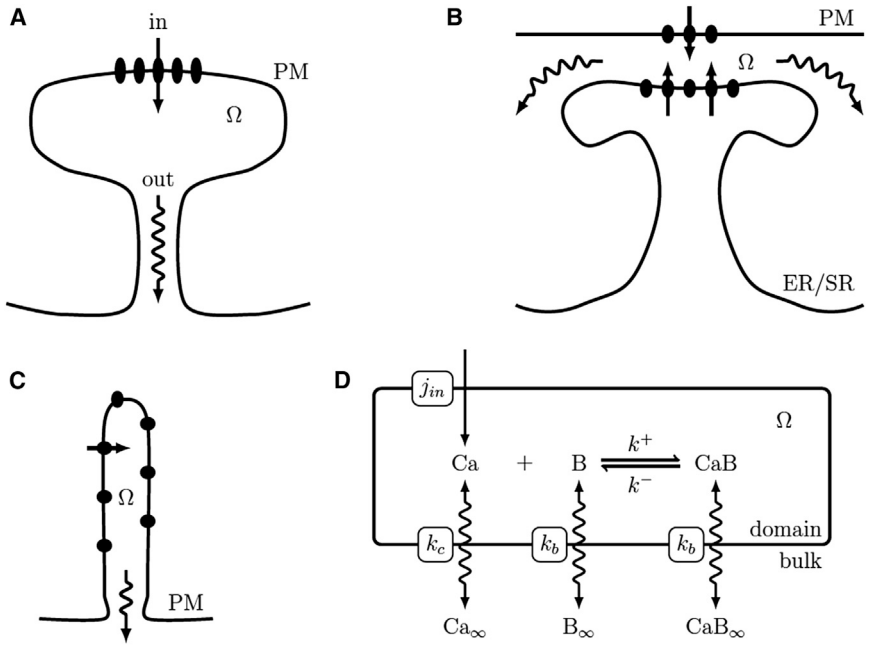

FIGURE 1 The analysis of the effect of Ca^{2+} buffers on domain $[Ca^{2+}]$ fluctuations is applicable to microdomains that arise from Ca^{2+} influx into a spatially restricted subcellular compartment. (*A*) In a dendritic spine (Ω denotes volume of spine head), Ca^{2+} influx occurs via ionotropic receptors (e.g., NMDA) or plasma membrane (PM) Ca^{2+} channels downstream of metabotropic receptors (e.g., mGluRs) (2). (*B*) In the cardiac dyad, Ca^{2+} influx via PM L-type Ca^{2+} channels trigger Ca^{2+} influx from Ca^{2+}-activated sarcoplasmic reticulum (SR) Ca^{2+} channels (ryanodine receptors) (7). Close associations of endoplasmic reticulum (ER) and PM are observed in many cell types. During ER depletion in Jurkat T cells, luminal Ca^{2+} sensor STIM1 aggregates on the ER membrane and binds the Ca^{2+} channel Orai1 providing store-operated Ca^{2+} entry. (*C*) In olfactory primary cilium, odorant detection induces a rise in second messenger cAMP, activating cyclic nucleotide-gated channels allowing entry of Ca^{2+} and Na^+ ions (11). (*D*) Model components and fluxes employed in the microdomain model. The stochastic ODE model includes Ca^{2+} influx, association of Ca^{2+} and buffer, and passive exchange of Ca^{2+} and buffer between the domain of volume Ω and the bulk cytosol.

MODEL FORMULATION

Domain $[Ca^{2+}]$ fluctuations in the absence of buffer

Deterministic ODE formulation

The deterministic ODE that minimally describes the time evolution of $[Ca^{2+}]$ in the domain depicted in Fig. 1 without buffer, constant influx j_{in}, and passive exchange with the bulk is

$$\dot{c} = j_{in} - k_c(c - c_\infty) \equiv f(c), \tag{6}$$

where k_c is the exchange rate (due to diffusion) that has physical dimensions of inverse time. Setting the left-hand side of Eq. 6 to zero, steady-state $[Ca^{2+}]$ is found to be

$$c_{ss} = j_{in}/k_c + c_\infty. \tag{7}$$

This deterministic formulation assumes that concentration fluctuations are negligible (i.e., large system size, $\Omega \to \infty$). The following section presents the corresponding stochastic ODEs that are valid for small domain volume.

Stochastic ODE (Langevin) formulation

In a domain with physical volume small enough that fluctuations are not negligible, but large enough that molecular concentrations can be modeled continuously, $[Ca^{2+}]$ dynamics may be described by a Langevin equation. This would be a stochastic differential equation (SDE) similar to the deterministic ODE (Eq. 6), but augmented by a fluctuating term, $\xi_c(t)$, with properties determined by the elementary molecular events that drive concentration fluctuations (26,37,38),

$$\dot{c} = f(c) + \xi_c(t). \tag{8}$$

In this stochastic ODE, $\xi_c(t)$ is Gaussian noise (specifically, a random function of time with zero mean),

$$\langle \xi_c(t) \rangle = 0 \tag{9}$$

and two-time covariance

$$\langle \xi_c(t)\xi_c(t') \rangle = \gamma_c \delta(t - t'), \tag{10}$$

where δ is the Dirac delta function and γ_c is given by

$$\gamma_c = \frac{j_{in} + k_c(c + c_\infty)}{\Omega}. \tag{11}$$

Note that the signs in the numerator are correct; γ_c is proportional to the sum of rates of the elementary processes leading to changes in $[Ca^{2+}]$, which includes increases through influx (j_{in}) as well as decreases and increases due to exchange with the bulk ($k_c c$ and $k_c c_\infty$). The reader who is unfamiliar with chemical Langevin equations may review the general form of the two-time covariance (see Appendix A in the Supporting Material).

Employing a linear noise approximation (26) for fluctuations around the stable steady-state c_{ss} transforms Eq. 8 into

$$\dot{\delta c} = -k_c \delta c + \xi_c^{ss}(t), \tag{12}$$

where δ_c is the deviation of the fluctuating [Ca^{2+}] from the steady-state value, c_{ss}, that is,

$$\delta c(t) = c(t) - c_{ss}, \tag{13}$$

and we have used $f'(c_{ss}) = -k_c$ and $\langle \xi_c^{ss}(t) \rangle = 0$. The two-time covariance of the random term takes the form

$$\left\langle \xi_c^{ss}(t)\xi_c^{ss}(t') \right\rangle = \gamma_c^{ss}\delta(t-t'),$$

where the constant γ_c^{ss} is found by evaluating Eq. 11 at steady state, that is,

$$\gamma_c^{ss} = \frac{2k_c c_{ss}}{\Omega}, \tag{14}$$

where we have used the balance of Ca^{2+} influx and efflux at steady state, $j_{in} = k_c(c_{ss} - c_\infty)$, to express the numerator as $2k_c c_{ss}$ rather than $j_{in} + k_c(c_{ss} + c_\infty)$ (compare to Eq. 14).

Analysis of concentration fluctuations

To understand the dynamics of [Ca^{2+}] fluctuations implied by Eq. 12, consider an ensemble of domains with initial state $c(0) = c_{ss}$, that is, $\delta_c(0) = 0$. The time evolution of the ensemble variance of the deviations δc, defined by $\sigma_c(t) = \langle \delta_c^2(t) \rangle$, follows from Eq. 12,

$$\dot{\sigma}_c = -2k_c\sigma_c + \gamma_c^{ss}, \tag{15}$$

where $k_c = |f'(c_{ss})|$ is the relaxation rate. By assumption, the ensemble variance is initially zero, that is, $\delta_c(0) = 0$ implies $\sigma_c(0) = 0$, but as time proceeds, $\sigma_c(t)$ is given by the solution of Eq. 15,

$$\sigma_c(t) = \sigma_c^0\left(1 - e^{-2k_c t}\right), \tag{16}$$

where steady-state ensemble variance σ_c^0 is found by setting $\dot{\sigma}_c = 0$ in Eq. 15,

$$\sigma_c^0 = \frac{\gamma_c^{ss}}{2k_c} = \frac{c_{ss}}{\Omega}. \tag{17}$$

The first equality in Eq. 17 relating σ_c^0 and γ_c^{ss} is called the "fluctuation-dissipation theorem" (25,26,39).

Thus, the relative size of the steady-state [Ca^{2+}] fluctuations in the Langevin formulation, given by the coefficient of variation of the fluctuating [Ca^{2+}], is

$$c_v^0 = \frac{\sqrt{\sigma_c^0}}{c_{ss}} = \frac{1}{\sqrt{c_{ss}\Omega}}. \tag{18}$$

Using the Langevin equation for a fluctuating Ca^{2+} microdomain, we have derived the well-known result (35) that the relative magnitude of concentration fluctuations is inversely proportional to the square-root of the system size, i.e., the expected number of Ca^{2+} ions in the domain at steady-state ($c_{ss}\Omega$). This result is a reference point for our analysis of domain [Ca^{2+}] fluctuations in the presence of buffer.

Domain [Ca^{2+}] fluctuations in the presence of buffer

Deterministic ODE formulation

In this section we characterize [Ca^{2+}] fluctuations in a domain model that includes Ca^{2+} buffers, Ca^{2+} influx, and exchange of both Ca^{2+} and buffer with the bulk (see Fig. 1). Assuming mass-action kinetics and bimolecular association of Ca^{2+} and buffer (Eq. 1), we write the following deterministic system of ODEs,

$$\dot{c} = R + j_{in} - k_c(c - c_\infty), \tag{19a}$$

$$\dot{b} = R - k_b(b - b_\infty), \tag{19b}$$

$$\dot{cb} = -R - k_b(cb - cb_\infty), \tag{19c}$$

where k_c and k_b are the Ca^{2+} and buffer exchange rates, and the reaction terms are given by $R = -k + c \times b + k - cb$, with c, b, and cb denoting free Ca^{2+}, free buffer, and bound buffer, respectively. We assume that the free and Ca^{2+}-bound buffer have the same exchange rate k_b and, furthermore, that the bulk concentrations b_∞ and cb_∞ are in equilibrium with the bulk free [Ca^{2+}],

$$b_\infty = \frac{\kappa b_T^\infty}{c_\infty + \kappa}, \text{ and}$$
$$cb_\infty = \frac{c_\infty b_T^\infty}{c_\infty + \kappa}.$$

Setting the time derivatives of Eq. 19 to 0, we find that the steady-state domain [Ca^{2+}], denoted by c_{ss}, solves the implicit expression

$$j_{in} - k_c(c_{ss} - c_\infty) - k_b(cb_{ss} - cb_\infty) = 0, \tag{20a}$$

where the steady-state Ca^{2+}-free and -bound buffer concentrations are given by

$$b_{ss} = \frac{\kappa b_T^\infty + k_b b_\infty/k_+}{c_{ss} + \kappa + k_b/k_+}, \text{ and}$$
$$cb_{ss} = \frac{c_{ss} b_T^\infty + k_b cb_\infty/k_+}{c_{ss} + \kappa + k_b/k_+}. \tag{20b}$$

In the presence of Ca^{2+} influx, $j_{in} > 0$, and because $\partial cb_{ss}/\partial c_{ss} > 0$, $c_{ss} > c_\infty$, $cb_{ss} > c_\infty$, and $b_{ss} > b_\infty$. Also note that $cb_{ss} + b_{ss} = b_T^\infty$ at this nonequilibrium steady state, because buffer in the bulk is at equilibrium, $cb_\infty + b_\infty = b_T^\infty$, and the exchange of Ca^{2+}-bound buffer

between domain and bulk, balances the exchange of Ca^{2+}-free buffer, $k_b(cb_{ss} - cb_\infty) = k_b(b_\infty - b_{ss}) > 0$.

Stochastic ODE (Langevin) formulation

As in the previous section, the Langevin-type stochastic Ca^{2+} domain model is found by adding the appropriate random terms to the deterministic ODEs (Eq. 19),

$$\dot{c} = R + j_{\text{in}} - k_c(c - c_\infty) + \xi_c(t), \tag{21a}$$

$$\dot{b} = R - k_b(b - b_\infty) + \xi_b(t), \tag{21b}$$

$$\dot{cb} = -R - k_b(cb - cb_\infty) + \xi_{cb}(t), \tag{21c}$$

where $\langle \xi_i(t) \rangle = 0$ for $i \in \{c,b,cb\}$. Because the $\xi_i(t)$ are correlated, the two-time covariances are most easily expressed in matrix form,

$$\left\langle \boldsymbol{\xi}(t)\boldsymbol{\xi}^T\left(t'\right)\right\rangle = \Gamma(c,b,cb)\delta\left(t - t'\right), \tag{22}$$

where $\boldsymbol{\xi}$ is the column vector $(\xi_c, \xi_b, \xi_{cb})^T$ and Γ is the state-dependent covariance matrix (see Appendix A in the Supporting Material),

$$\Gamma(c,b,cb) = \begin{pmatrix} \gamma_r + \gamma_c & \gamma_r & -\gamma_r \\ \gamma_r & \gamma_r + \gamma_b & -\gamma_r \\ -\gamma_r & -\gamma_r & \gamma_r + \gamma_{cb} \end{pmatrix}, \tag{23a}$$

where

$$\begin{aligned} \gamma_r(c,b,cb) &= \frac{k_+c \times b + k_-cb}{\Omega}, \\ \gamma_c(c) &= \frac{j_{\text{in}} + k_c(c + c_\infty)}{\Omega}, \\ \gamma_b(b) &= \frac{k_b(b + b_\infty)}{\Omega}, \\ \gamma_{cb}(cb) &= \frac{k_b(cb + cb_\infty)}{\Omega}. \end{aligned} \tag{23b}$$

Denoting the fluctuations around steady state by $\delta c = c - c_{ss}$, $\delta b = b - b_{ss}$, and $\delta cb = cb - cb_{ss}$, the linear SDE system for the concentration fluctuations in the presence of buffer is

$$\dot{\boldsymbol{\delta}} = H_{ss}\,\boldsymbol{\delta} + \boldsymbol{\xi}_{ss}(t), \tag{24}$$

where $\boldsymbol{\delta} = (\delta c, \delta c, \delta cb)^T$ is a column vector, H_{ss} is the Jacobian of the full system of SDEs evaluated at steady state,

$$H_{ss} = \begin{pmatrix} -k_+b_{ss} - k_c & -k_+c_{ss} & k_- \\ -k_+b_{ss} & -k_+c_{ss} - k_b & k_- \\ k_+b_{ss} & k_+c_{ss} & -k_- - k_b \end{pmatrix},$$

$\langle \xi_{ss}(t) \rangle = 0$, and $\langle \xi_{ss}(t)\ \xi^T{}_{ss}(t') \rangle = \Gamma_{ss}\delta(t - t')$ with steady-state covariance matrix (compare to Eq. 23),

$$\Gamma_{ss} = \begin{pmatrix} \gamma_r^{ss} + \gamma_c^{ss} & \gamma_r^{ss} & -\gamma_r^{ss} \\ \gamma_r^{ss} & \gamma_r^{ss} + \gamma_b^{ss} & -\gamma_r^{ss} \\ -\gamma_r^{ss} & -\gamma_r^{ss} & \gamma_r^{ss} + \gamma_{cb}^{ss} \end{pmatrix}, \tag{25a}$$

where

$$\begin{aligned} \gamma_r^{ss} &= \frac{k_+c_{ss} \times b_{ss} + k_-cb_{ss}}{\Omega}, \\ \gamma_c^{ss} &= \frac{j_{\text{in}} + k_c(c_{ss} + c_\infty)}{\Omega}, \\ \gamma_b^{ss} &= \frac{k_b(b_{ss} + b_\infty)}{\Omega}, \\ \gamma_{cb}^{ss} &= \frac{k_b(cb_{ss} + cb_\infty)}{\Omega}. \end{aligned} \tag{25b}$$

If one prefers, the Langevin system for the fluctuations (Eq. 24) can be written as

$$\dot{\delta c} = -(k_+b_{ss} + k_c)\,\delta c - k_+c_{ss}\,\delta b + k_-\,\delta cb + \xi_c^{ss}(t), \tag{26a}$$

$$\dot{\delta b} = -k_+b_{ss}\,\delta c - (k_+c_{ss} + k_b)\,\delta b + k_-\,\delta cb + \xi_b^{ss}(t), \tag{26b}$$

$$\dot{\delta cb} = k_+b_{ss}\,\delta c + k_+c_{ss}\,\delta b - (k_- + k_b)\,\delta cb + \xi_{cb}^{ss}(t). \tag{26c}$$

Analysis of concentration fluctuations

Our analysis of concentration fluctuations in the presence of buffer begins by defining a symmetric 3×3 covariance matrix for the fluctuating concentrations, $\Sigma(t) = (\sigma_{ij})$ for i, $j \in \{c,b,cb\}$, that is,

$$\Sigma(t) = \left\langle \boldsymbol{\delta}(t)\boldsymbol{\delta}^T(t)\right\rangle = \begin{pmatrix} \langle \delta c^2 \rangle & \langle \delta c\,\delta b \rangle & \langle \delta c\,\delta cb \rangle \\ \bigstar & \langle \delta b^2 \rangle & \langle \delta b\,\delta cb \rangle \\ \bigstar & \bigstar & \langle \delta cb^2 \rangle \end{pmatrix},$$

where each star indicates a redundant entry. The time-dependent dynamics of $\Sigma(t)$ follows from Eq. 24 (26),

$$\dot{\Sigma} = H_{ss}\Sigma + \Sigma H_{ss}^T + \Gamma_{ss}, \tag{27}$$

which is the matrix version of Eq. 15. Solving Eq. 27 with the initial condition $\Sigma(0) = 0$ corresponds to an ensemble of domains with initial state $c(0) = c_{ss}$, $b(0) = b_{ss}$, and $cb(0) = cb_{ss}$, that is, $\delta c = \delta b = \delta cb = 0$. This equation represents a linear system of 6 ODEs simultaneously solved by the six covariances $\langle \delta c^2 \rangle$, $\langle \delta c \delta b \rangle$,…, $\langle \delta cb^2 \rangle$.

The covariances $\Sigma(t)$ that solve Eq. 27 are the focus of this article's mathematical and computational analysis of domain $[Ca^{2+}]$ fluctuations in the presence of buffer. The solution of Eq. 27 with $\Sigma(0) = 0$ is (26),

$$\Sigma(t) = \int_0^t \exp(H_{ss}\hat{t})\Gamma_{ss}\exp\left(H_{ss}^T\hat{t}\right)d\hat{t}. \tag{28}$$

The steady-state ensemble variance is the limiting value of this expression as $t \to \infty$,

$$\Sigma_{ss} = \int_0^\infty \exp(H_{ss}t)\Gamma_{ss}\exp\left(H_{ss}^T t\right)dt, \tag{29}$$

but the steady-state ensemble variance Σ_{ss} is often more conveniently found by solving the linear algebraic system for the steady state of Eq. 27, the continuous Lyapunov equation, and the more general form of the fluctuation-dissipation theorem,

$$H_{ss}\Sigma_{ss} + \Sigma_{ss}H_{ss}^T = -\Gamma_{ss}. \tag{30}$$

Equation 30 can be solved numerically using the command LYAP available in the software MATLAB (The MathWorks, Natick, MA). For symbolic and analytical calculations, we rewrite Eq. 30 as

$$(H_{ss} \oplus H_{ss})\mathrm{vec}(\Sigma_{ss}) = -\mathrm{vec}(\Gamma_{ss}) \tag{31}$$

and then expand in terms of the parameters of the problem and the unknown entries of Σ_{ss}. In Eq. 31, I is the 3×3 identity matrix, $H_{ss} \oplus H_{ss}$ is a Kronecker sum given by

$$H_{ss} \oplus H_{ss} = I \otimes H_{ss} + H_{ss} \otimes I,$$

where $\otimes$ is the Kronecker product, the vec operation creates a column vector from a matrix by stacking its column vectors, and we have used

$$\mathrm{vec}(AB) = (I \otimes A)\mathrm{vec}(B) = \left(B^T \otimes I\right)\mathrm{vec}(A).$$

Although $H_{ss} \otimes H_{ss}$ is 9×9 and $\mathrm{vec}(\Sigma_{ss})$ and $\mathrm{vec}(\Gamma_{ss})$ are 9×1, Σ_{ss} and Γ_{ss} are symmetric and thus Eq. 31 can be contracted to a 6×6 linear system by eliminating rows 4, 7, and 8 of $\mathrm{vec}(\Sigma_{ss})$ and $\mathrm{vec}(\Gamma_{ss})$ and the corresponding rows and columns of the $H_{ss} \oplus H_{ss}$.

The remainder of this article communicates numerical and analytical results obtained using this Langevin formulation for domain [Ca^{2+}] fluctuations in the presence of buffer.

RESULTS

The influence of Ca^{2+} buffers on domain [Ca^{2+}] fluctuations

Fig. 2 shows parameter studies that characterize the dependence of the relative magnitude of domain [Ca^{2+}] fluctuations on Ca^{2+} buffer parameters. Results were obtained by numerically solving the continuous Lyapunov equation (Eq. 30) for a range of total buffer concentrations (b_T^∞) and rate constants (k_+ and k_-), fast and slow exchange rates for Ca^{2+}-free and -bound buffer with the bulk (k_b), and Ca^{2+} influx rates leading to steady-state free [Ca^{2+}] of $c_{ss} = 1$, 10, and 100 μM. The relative magnitude of domain [Ca^{2+}] fluctuations are characterized by the coefficient of variation

$$c_v = \frac{\sqrt{\sigma_c^{ss}}}{c_{ss}}, \tag{32}$$

where the steady-state domain concentration c_{ss} is determined by the Ca^{2+} influx rate via Eq. 20 and $\sigma_c^{ss} = \langle \delta c^2 \rangle_{ss}$ is the germane element of Σ_{ss} found by numerical solution of Eq. 30. Numerically calculated c_v values that were generated from Monte Carlo simulations of an ensemble of domains using Gillespie's stochastic simulation algorithm (40) agree with the linear noise approximation, validating our approach (see Fig. S1 in the Supporting Material).

Fig. 2 reveals that the relative magnitude of domain [Ca^{2+}] fluctuations (c_v) is a biphasic (bell-shaped) function of the total buffer concentration b_T^∞ (*gray lines*). For small

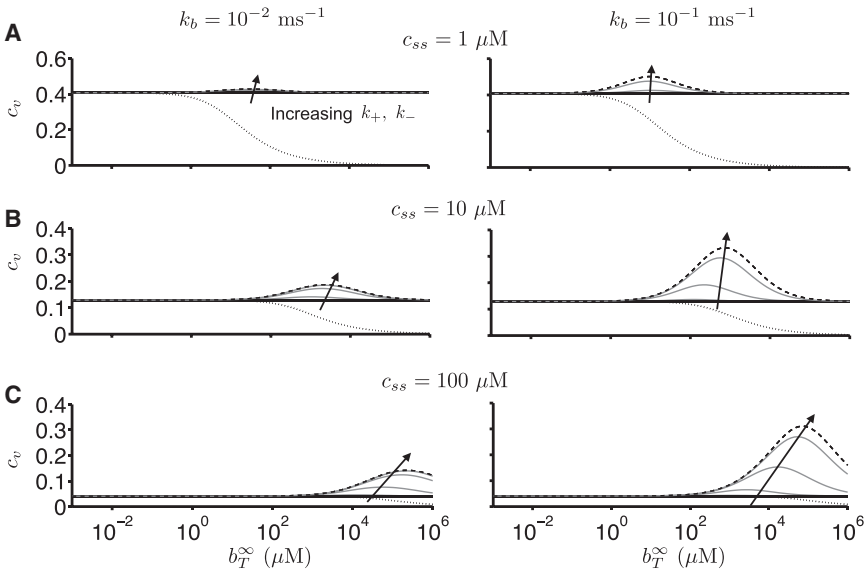

FIGURE 2 Dependence of the relative magnitude of domain [Ca^{2+}] fluctuations probed by plotting the coefficient of variation (c_v) of the deviation of the fluctuating [Ca^{2+}] on buffer parameters. (*Shaded lines*) c_v for different values of buffer binding reaction rate k_+. (*Solid lines*) c_v^0 in the absence of buffer (Eq. 5). (*Dotted line*) c_v predicted from a naive application of the concept of effective volume employed in deterministic models of Ca^{2+} signaling (Eq. 33). (*Dashed lines*) c_v', the (correctly derived) influence of buffer on c_v in the rapid buffer limit (Eq. 39). Parameters: $c_{ss} = 1$ (*A*), 10 (*B*), and 100 (*C*) μM, $c_\infty = 0.1$ μM, $\kappa = 0.2$ μM, $k_c = 0.2$ ms^{-1}, $k_+ = 10^{-3}$, and 1 μM^{-1} ms^{-1}. The domain volume $\Omega = 10^{-17}$ L corresponds to 0.01 $\mu m^3 \approx (0.22\ \mu m)^3$.

or large total buffer concentrations (b_T^∞), the relative fluctuation magnitude (c_v) asymptotically approaches the value obtained in the absence of buffer ($c_v^0 = 1/\sqrt{c_{ss}\Omega}$, *solid black line*). This asymptotic value represents the minimum fluctuation size; c_v is enhanced for intermediate total buffer concentrations. Rapid Ca^{2+} buffers increase the relative fluctuation magnitude, that is, for fixed $\kappa = k_-/k_+$, the c_v increases with increasing k_+. High mobility Ca^{2+} buffer (represented in this compartmental formulation by increasing the exchange rate k_b) also enhances domain $[Ca^{2+}]$ fluctuations (compare *left* and *right columns*). High Ca^{2+} influx rates (j_{in}) amplify domain $[Ca^{2+}]$ fluctuations for intermediate, but not extreme, concentrations of buffer. Taken together, these results indicate that domain $[Ca^{2+}]$ fluctuations are significantly enhanced by Ca^{2+} buffer and nontrivially dependent on Ca^{2+} buffer properties.

The response of domain $[Ca^{2+}]$ to buffer parameters documented in Fig. 2 are counterintuitive in the sense that our numerical calculations are precisely the opposite of what one would predict using a naive application of the concept of effective volume. As mentioned in the Introduction, the effective volume derived from the rapid buffer limit of the deterministic equations for buffered Ca^{2+} dynamics (Eq. 19) is $\Omega_{eff} = \Omega/\beta$, where the buffering factor β is given by Eq. 3. If one replaces the physical volume Ω in Eq. 18 with this effective volume, one might conjecture that

$$c_v \stackrel{?}{=} \frac{1}{\sqrt{c_{ss}\Omega_{eff}}} = \sqrt{\frac{\beta_{ss}}{c_{ss}\Omega}}, \tag{33}$$

where $\beta_{ss} = \beta(c_{ss})$. However, the numerical calculations presented in Fig. 2 show that this is incorrect (*dotted line*). In fact, this naive application of the concept of buffer-mediated increase in effective volume is quite misleading. Comparison of solid and dotted lines in Fig. 2 show that Eq. 33 incorrectly suggests that the size of $[Ca^{2+}]$ fluctuations is suppressed by buffer (by increasing the system size, $c_{ss}\Omega_{eff} > c_{ss}\Omega$). The conjecture of Eq. 33 also incorrectly suggests that domain $[Ca^{2+}]$ fluctuations can be eliminated ($c_v \to 0$) as total buffer concentration b_T^∞ increases and drives the differential fraction of free to total calcium to zero ($\beta_{ss} \to 0$). On the contrary, the numerical results of this section (and analytical results presented below) are definitive*:* during periods of Ca^{2+} influx, Ca^{2+} buffers enhance domain $[Ca^{2+}]$ fluctuations.

The size of $[Ca^{2+}]$ fluctuations in the rapid buffer limit

Although closed-form analytical solution for the entries of the steady-state covariances Σ_{ss} (and in particular σ_c^{ss}) can be obtained beginning with Eq. 31, the algebra is tedious, the result is unwieldy, and little insight is gained from these expressions (not shown). On the other hand, numerical evaluation of symbolic solutions of Eq. 31 confirm the results of the previous section obtained by numerically solving the Lyapunov equation (Eq. 30).

To obtain more insight into the enhancement of domain $[Ca^{2+}]$ fluctuations mediated by Ca^{2+} buffers, we sought to derive a stochastic version of the rapid buffer approximation (RBA) that correctly accounts for the influence of fast Ca^{2+} buffering on domain $[Ca^{2+}]$ fluctuations. Two distinct approaches were identified and successfully employed, both yielding the same analytical result. In the first approach, the above-mentioned cumbersome analytical expression for σ_c^{ss} was symbolically evaluated in the limit that $k_+, k_- \to \infty$ for fixed $\kappa = k_-/k_+$. The second approach involves no symbolic computations, but rather implements a general method for deriving a 0th-order approximation to the size of fluctuations in chemical reaction networks with widely separated timescales (26).

Briefly, beginning with the stochastic ODEs for buffered Ca^{2+} dynamics (Eq. 26), we identify the fluctuations in total calcium ($\delta c_T = \delta c + \delta cb$) and total buffer ($\delta b_T = \delta b + \delta cb$) as the slow variables. Differentiating these expressions and adding equations, we obtain the fast/slow system

$$\begin{aligned}\dot{\delta c} =& -[k_+(c_{ss}+b_{ss})+k_-+k_c]\delta c+(k_+c_{ss}+k_-)\delta c_T \\ & - k_+c_{ss}\,\delta b_T+\xi_c^{ss}(t),\end{aligned} \tag{34a}$$

$$\dot{\delta c}_T = -(k_c-k_b)\delta c - k_b\,\delta c_T + \xi_{c_T}^{ss}(t), \tag{34b}$$

$$\dot{\delta b}_T = -k_b\delta b_T + \xi_{b_T}^{ss}(t), \tag{34c}$$

where δc is the fast variable, δc_T and δb_T are slow variables, and we define

$$\xi_{c_T}^{ss}(t) = \xi_c^{ss}(t) + \xi_{cb}^{ss}(t) \text{ and } \xi_{b_T}^{ss}(t) = \xi_b^{ss}(t) + \xi_{cb}^{ss}(t).$$

In the rapid buffer limit ($k_+, k_- \to \infty$ with $\kappa = k_-/k_+$ fixed), a quasistatic approximation for the average value of the $[Ca^{2+}]$ fluctuation that is valid on the slow (outer) timescale is

$$\langle\delta c\rangle_* \approx \beta_{ss}[\delta c_T - \nu_{ss}\,\delta b_T], \tag{35}$$

where we have written $\nu_{ss} = c_{ss}/(c_{ss}+\kappa)$, and $\langle\bullet\rangle_*$ indicates a time average (as opposed to an ensemble average) and we have used the fact that $b_{ss} \to b_T\kappa/(c_{ss}+\kappa)$ in the RBA limit (compare to Eq. 20b). Replacing δc in the slow equations by this average value gives

$$\dot{\delta c}_T = -\beta_{ss}(k_c + w_{ss}k_b)\delta c_T + \beta_{ss}(k_c-k_b)\nu_{ss}\,\delta b_T + \xi_{c_T}^{ss}(t), \tag{36a}$$

$$\dot{\delta b}_T = -k_b\delta b_T + \xi_{b_T}^{ss}(t), \tag{36b}$$

thereby expressing the slow SDEs in terms of δc_T and δb_T. Next, the 2×2 covariance matrix Γ_{ss}^{slow} for $\xi_{c_T}^{ss}$ and $\xi_{b_T}^{ss}$ is

calculated, and the 2×2 matrix Σ_{ss}^{slow}, whose entries correspond to $\langle \delta c_T^2 \rangle$, $\langle \delta c_T \delta b_T \rangle$, and $\langle \delta b_T^2 \rangle$, is found by solving a 2×2 Lyapunov equation (Eq. 30). Finally, the values of $\langle \delta c^2 \rangle$, $\langle \delta c \delta c_T \rangle$, and $\langle \delta c \delta b_T \rangle$ consistent with Eq. 34 are found by solving a 3×3 Lyapunov equation for $\langle \delta c^2 \rangle$, $\langle \delta c \delta c_T \rangle$, and $\langle \delta c \delta b_T \rangle$. From the perspective of analytical work, this two-step process is far easier than solving the Lyapunov equation for the covariance matrix Σ_{ss} for δc, δb, and δcb, because the fast and slow versions of the Γ_{ss} and H_{ss} matrices are simpler than those that appear in the full calculation (see Appendix B in the Supporting Material for details).

Using both of the above-mentioned approaches (symbolic and analytical), we find that the variance of the free [Ca^{2+}] fluctuations in the presence of rapid Ca^{2+} buffer (denoted by σ_c') is given by

$$\begin{aligned} \sigma_c' &= \frac{c_{ss}}{\Omega} \times (1+\chi), \\ \chi &= \beta_{ss} \times \frac{w_{ss} k_b}{k_c + w_{ss} k_b} \times \frac{c_{ss} - c_\infty}{\kappa + c_\infty}, \end{aligned} \tag{37}$$

where β_{ss} and w_{ss} are evaluated at the steady-state domain [Ca^{2+}],

$$\begin{aligned} \beta_{ss} &= \frac{1}{1+w_{ss}}, \\ w_{ss} &= \frac{b_T^\infty \kappa}{(c_{ss}+\kappa)^2}, \end{aligned} \tag{38}$$

and we note that $c_{ss} \geq c_\infty$ and thus $\chi \geq 0$. The variance σ_c' implies that in the rapid buffer limit the coefficient of variation for domain [Ca^{2+}] fluctuations is given by

$$c_v' = \frac{\sqrt{\sigma_c'}}{c_{ss}} = \sqrt{\frac{1+\chi}{c_{ss}\Omega}} = c_v^0 \sqrt{1+\chi}, \tag{39}$$

where $c_v^0 = 1/\sqrt{c_{ss}\Omega}$ is the result in absence of buffer. Noting that $\chi \geq 0$, we find

$$\frac{c_v'}{c_v^0} = \sqrt{1+\chi} \geq 1 \tag{40}$$

and conclude that Ca^{2+} buffers may enhance but cannot suppress domain [Ca^{2+}] fluctuations.

One way to represent the effect of rapid buffers on domain [Ca^{2+}] fluctuations involves rewriting Eq. 37 as

$$\begin{aligned} \sigma_c' &= \frac{c_{ss}}{\Omega_{\text{eff}}'}, \\ \Omega_{\text{eff}}' &= \frac{\Omega}{1+\chi}, \end{aligned} \tag{41}$$

where Ω'_{eff} denotes an effective volume that appropriately accounts for the influence of rapid Ca^{2+} buffers on [Ca^{2+}] fluctuations. The fluctuating RBA is readily generalizable to multiple buffers (see Eq. S1 in the Supporting Material). We show that domain [Ca^{2+}] fluctuations in the presence of two rapid buffers with different dissociation constants and exchange rates is given by the multiple buffer fluctuating RBA and not a naive weighted average utilizing total buffer concentration (see Fig. S2 in the Supporting Material).

Interpretation of the fluctuating rapid buffer limit

Some salient observations can be made regarding domain [Ca^{2+}] fluctuations in the rapid buffer limit (Eqs. 37 and 41):

1. The effective volume in the fluctuating RBA is smaller than the physical volume ($\chi \geq 0$ and thus $\Omega'_{\text{eff}} \leq \Omega$). This is in marked contrast to the effective volume for the deterministic RBA that is greater than the physical volume ($\Omega'_{\text{eff}} = \Omega/\beta_{ss} > \Omega$). This is to say, we have analytically confirmed our previous numerical result demonstrating that rapid buffers typically increase the magnitude of domain [Ca^{2+}] fluctuations (Fig. 2).
2. The χ in σ_c' is proportional to the concentration difference $c_{ss} - c_\infty$ (Eq. 37). That is, the buffer-mediated enhancement of domain [Ca^{2+}] fluctuations is an increasing function of the disequilibrium between the steady-state domain [Ca^{2+}] (c_{ss}) and the bulk (c_∞).
3. The numerically observed biphasic dependence of the relative magnitude of domain [Ca^{2+}] fluctuations (c_v in Fig. 2) corresponds to the factor $\beta_{ss} w_{ss} k_b/(k_c + w_{ss} k_b)$ in χ that is a biphasic function of b_T^∞ through β_{ss} and w_{ss}.
4. In several limiting parameter regimes, the steady-state variance of domain [Ca^{2+}] fluctuations is not affected by Ca^{2+} buffer ($\chi = 0$ and thus $\sigma_c' = \sigma_c^0 = c_{ss}/\Omega$). These include the absence of Ca^{2+} influx ($j_{\text{in}} = 0$, $c_{ss} = c_\infty$), immobile buffer that is unable to exchange with the bulk ($k_b = 0$), and extreme values for the total buffer concentration (both $b_T^\infty \to 0$ and $b_T^\infty \to \infty$). However, even in these limiting parameter regimes, buffers do not decrease [Ca^{2+}] fluctuations to a size less than that observed in the absence of buffer.
5. The total buffer concentration that maximizes domain [Ca^{2+}] fluctuations for a given fixed c_{ss},

$$b_{T*}^\infty = \sqrt{\frac{k_c}{k_b}} \times \frac{(c_{ss}+\kappa)^2}{\kappa}, \tag{42}$$

is found as the b_T^∞ that zeros $\partial(1+\chi)/\partial b_T^\infty = \partial\chi/\partial b_T^\infty$. This corresponds to

$$w_{ss}^* = \sqrt{k_c/k_b},$$

$$\beta_{ss}^* = \sqrt{k_b/k_c} \Big/ \left(1 + \sqrt{k_b/k_c}\right),$$

and

$$\Omega'^{*}_{\text{eff}} = \frac{\Omega}{1+\chi^{*}},$$
$$c'^{*}_{v} = \sqrt{\frac{1+\chi^{*}}{c_{ss}\Omega}}, \tag{43}$$
$$\chi^{*} = \frac{k_b/k_c}{\left(1+\sqrt{k_b/k_c}\right)^2} \times \frac{c_{ss}-c_{\infty}}{\kappa + c_{\infty}}.$$

6. Equation 43 indicates that the maximum fluctuation magnitude is determined in part by the relative exchange rate k_b/k_c. Because χ^* is a monotone increasing function of k_b/k_c, domain $[Ca^{2+}]$ fluctuations can, formally, be made as large as possible by choosing $k_b \gg k_c$ and optimal b^{∞}_{T*} (Eq. 42). However, the molecular weight of Ca^{2+}-bound buffer is greater than Ca^{2+} and, consequently, one expects Ca^{2+}-bound buffer to diffuse and exchange with the bulk more slowly than free Ca^{2+}. This physical consideration implies that $k_b \leq k_c$ and, after imposing this constraint, the physiologically realistic parameter choice that maximizes domain $[Ca^{2+}]$ fluctuations ($k_b \approx k_c$) leads to $\chi^* \approx 1/4(c_{ss} - c_{\infty})/(c_{\infty} + \kappa)$ and thus
$$\left.\frac{c'_v}{c^0_v}\right|_{*} = \sqrt{1+\frac{c_{ss}-c_{\infty}}{4(c_{\infty}+\kappa)}}.$$
7. The buffer dissociation constant κ influences buffer-mediated increase in $[Ca^{2+}]$ fluctuations in a complex manner. For example, the variance of free $[Ca^{2+}]$ fluctuations (σ'_c, Eqs. 37 and 38) depends on the relative (as opposed to absolute) concentrations of domain (c_{ss}/κ) and bulk (c_{∞}/κ) Ca^{2+} and total buffer (b^{∞}_T/κ) via the dimensionless quantities β_{ss} and w_{ss}. This is because the buffering capacity can expressed as $w_{ss} = (b^{\infty}_T/\kappa)/(1 + c_{ss}/\kappa)^2$ and, similarly, the second factor of χ can be written as $(c_{ss}/\kappa - c_{\infty}/\kappa)/(1 + c_{\infty}/\kappa)$. For a given steady-state $[Ca^{2+}]$, c_{ss}, the total buffer concentration with maximal effect (b^{∞}_{T*}, Eq. 42) is a u-shaped function of the buffer dissociation constant κ (see Supporting Results and Fig. S3 in the Supporting Material).

Applicability of the fluctuating rapid buffer approximation

In the spatial and deterministic formulation of the buffered diffusion of intracellular Ca^{2+}, the rapid buffer approximation is valid when the equilibration time for buffers is much smaller than the time constant for Ca^{2+} diffusion. In this minimal model of domain $[Ca^{2+}]$ fluctuations, Ca^{2+} and buffer diffusion are represented as first-order reactions (rate constants k_c and k_b) that couple the domain with the bulk. The validity of the fluctuating RBA depends on buffer kinetics being faster than exchange. Consequently, the physical domain volume influences the validity of this approximate result.

The time constant for diffusion-mediated passive exchange between compartments can be characterized by the mean escape time for a Brownian particle with diffusion constant D leaving a domain of volume Ω via a small opening of radius a (36),

$$\tau = \frac{\Omega}{4aD}. \tag{44}$$

As illustrated in Fig. 3 *A*, a cubical domain ($\Omega = L^3$) with an opening whose radius scales with linear dimension ($\rho = a/L < 1$) would yield rate constant $k = 1/\tau$ and thus $k_i = 4\rho D_i/L^2$, where $i \in \{c, b\}$ and D_c and D_b are the diffusion coefficients for Ca^{2+} and buffer, respectively. Using parameters for the fast, mobile buffer BAPTA, Fig. 3 *B* plots the coefficient of variation of domain $[Ca^{2+}]$ fluctuations (c_v) and the buffer-mediated relative decrease in system size (σ^0_c/σ^{ss}_c, where $\sigma^0_c = c_{ss}/\Omega$) as functions of physical domain volume Ω for different values of the dimensionless escape radius ρ (*shaded lines*). As expected, both c_v and σ^0_c/σ^{ss}_c decrease with system size Ω. Narrowing the dimensionless escape radius (decreasing ρ) leads to an increase in c_v and a decrease in σ^0_c/σ^{ss}_c for any physical domain volume Ω. Comparison of the solid and dotted lines in Fig. 3 *B* shows that the fluctuating RBA agrees with the full calculation when the physical domain volume Ω is sufficiently large and/or the escape opening is sufficiently narrow (small ρ). Both situations lead to exchange rates (k_c and k_b) that are small compared to rate of buffer equilibration (an increasing function of both k_+ and k_-).

$[Ca^{2+}]$ fluctuations in a physiological setting

Neuronal dendritic spines are a good setting to illustrate the influence of Ca^{2+} buffer on domain $[Ca^{2+}]$ fluctuations and explore the validity of the fluctuating RBA, in part because such spines are highly variable in shape and size. Although it is difficult to define an average spine geometry, most spines have a clearly defined neck (corresponding to the escape opening of radius a in the previous paragraph) and head (corresponding to the microdomain of volume Ω). Fig. 3 *C* illustrates three frequently observed spine shapes—thin, mushroom, and stubby—whose geometric parameters (a and Ω) have been experimentally quantified (41).

Fig. 3 *D* shows that over a wide range of concentrations, the fast buffer BAPTA increases the coefficient of variation, compared with the absence of buffer (c_v/c^0_v), by as much as a factor of 2 (*top*). The largest increase occurs in the case of the mushroom-shaped dendritic spine, for which the ratio of the spine-neck opening cross-sectional area, and the spine-head volume, is smallest (a/Ω).

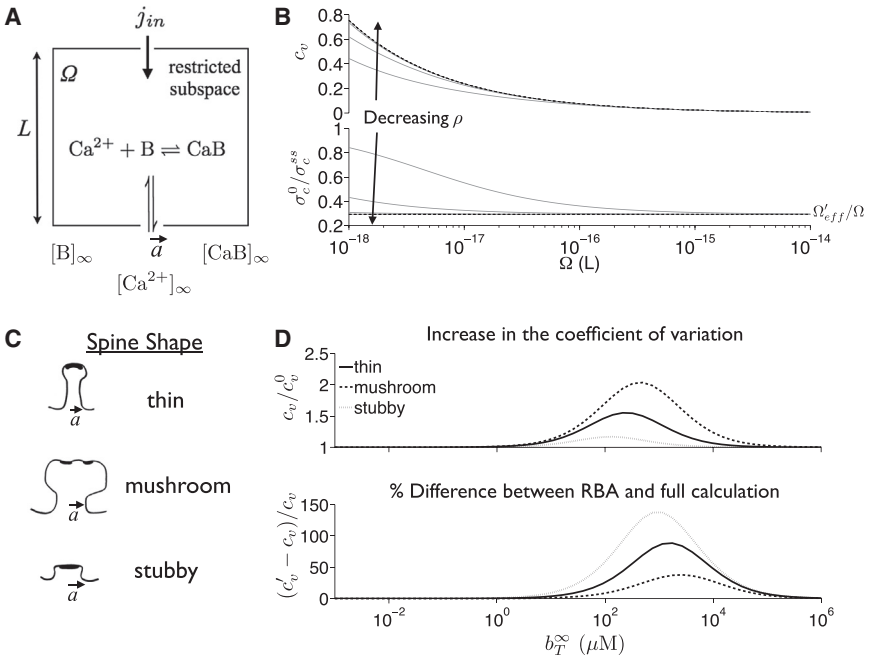

FIGURE 3 The geometric parameters of a Ca^{2+} domain determine the time constant for escape of Ca^{2+} and buffer and the range of applicability of the fluctuating rapid buffer approximation (RBA). (*A*) Diagram of restricted subspace with volume Ω, linear dimension L, and radius of domain escape a. (*B*) (*Shaded lines*) Coefficient of variation of domain $[Ca^{2+}]$ fluctuations (c_v, *top*) and buffer-mediated relative decrease in system size (σ_c^0/σ_c^{ss}, *bottom*) as functions of physical domain volume Ω using four decades of dimensionless escape radii $\rho = a/L = 10^{-4},\ldots,10^{-1}$. (*Dashed black lines*) Fluctuating RBA (Eq. 39) well approximates the full calculation when ρ is small. $c_{ss} = 1$ μM. (*C*) Illustration of three frequent spine shapes adapted from Harris et al. (41). (*D*, *top*) Relative increase in c_v in the presence of BAPTA, compared with the absence of buffer c_v^0, for different spine shapes. (*D*, *bottom*) Percent difference between c_v as calculated using the fluctuating RBA, c'_v and the full calculation, c_v. $c_{ss} = 10$ μM. Parameters: $c_\infty = 0.1$ μM, $D_c = 0.2$ μm^2/ms. BAPTA (72): $D_b = 0.1$ μm^2/ms, $k_+ = 0.6$ μM^{-1} ms^{-1}, $\kappa = 0.2$ μM, and $b_T^\infty = 100$ μM. Spine geometries (41): thin ($a = 0.05$ μm, $\Omega = 4 \times 10^{-17}$ L), mushroom ($a = 0.1$ μm, $\Omega = 2.9 \times 10^{-16}$ L), and stubby ($a = 0.16$ μm, $\Omega = 3 \times 10^{-17}$ L).

For small and large BAPTA concentrations, there is a negligible difference between the fluctuating RBA and the corresponding full calculation, even measured in relative terms (Fig. 3 *D*, *bottom*). When the BAPTA concentration induces comparatively large $[Ca^{2+}]$ fluctuations, the fluctuating RBA overestimates the c_v (depending on spine shape by as much as 50–150% in the worst case). When the steady-state domain $[Ca^{2+}]$ (c_{ss}) is decreased, the disequilibrium between domain Ca^{2+} and buffer is attenuated, and the relative deviation between the RBA and full calculation is smaller (not shown). The fluctuating RBA works best for the mushroom-shaped dendritic spine, because a/Ω is smallest.

Influence of buffers on the relaxation time for domain $[Ca^{2+}]$ fluctuations

We have demonstrated that in the presence of Ca^{2+} influx ($j_{in} > 0$), Ca^{2+} buffer may significantly increase the steady-state covariance of $[Ca^{2+}]$ fluctuations, especially when buffers are mobile and rapid (Eq. 37). On the other hand, the fluctuating RBA shows that in the absence of Ca^{2+} influx ($j_{in} = 0$, $c_{ss} = c_\infty$), fluctuation amplitude is not influenced by total buffer concentration ($c_v = c_v^0 = 1/\sqrt{c_{ss}\Omega}$ as when $b_T^\infty = 0$), a result that holds generally (e.g., when buffers are slow) in numerical simulations (not shown). This occurs because Γ_{ss} and H_{ss} scale in such a way that the steady-state covariance matrix Σ_{ss} is not a function of b_T^∞ when $j_{in} = 0$ (Eq. 30). On the other hand, the time-dependent stochastic dynamics of the fluctuating concentrations (δc, δb, δcb) and the relaxation of the covariance matrix Σ to steady state are a function of buffer properties in both the absence or presence of Ca^{2+} influx (Eq. 27). For example, the relaxation rates governing the dynamics of Eq. 27 are given by the pairwise sums of the eigenvalues of H_{ss} (by properties of Kronecker sums and Eq. 31 (42)), and these are a function of b_T^∞ in both the presence and absence of Ca^{2+} influx.

Fig. 4 *A* shows Monte Carlo simulations of domain $[Ca^{2+}]$, $c(t)$, fluctuating around the steady-state c_{ss} that were generated by numerical integration of Eq. 21 using the Euler-Maruyama method. In the absence of buffer, the fluctuations $\delta_c(t) = c(t) - c_{ss}$ are typically small and long-lasting (Fig. 4 *Aa*). Similar dynamics are observed in the presence of slow buffers (Fig. 4 *Ab*). Conversely, in the presence of rapid buffer, free $[Ca^{2+}]$ fluctuations and subsequent relaxation to steady state occurs on a fast timescale (Fig. 4 *Ac*).

One characterization of the influence of buffer on the time evolution of $[Ca^{2+}]$ fluctuations is given by the 3×3 steady-state correlation function $\Phi = (\phi_{i,j})$ with $i,j \in \{c,b,cb\}$,

$$\Phi(\tau) \equiv \left\langle \boldsymbol{\delta}(\tau)\boldsymbol{\delta}^T(0) \right\rangle,$$

where $\Phi(0) = \Sigma_{ss}$. In the presence of buffer the correlation function for the domain $[Ca^{2+}]$ fluctuation δc is given by $\phi_{c,c}(\tau)$, where $-\infty < \tau < \infty$ and

$$\Phi(\tau) = \exp(-|\tau|H_{ss})\Sigma_{ss}, \tag{45}$$

whereas in the absence of buffer $\phi^0_{c,c}(\tau) = \sigma_c^0 \exp(-k_c|\tau|)$ (26). Fig. 4 *B* plots $\phi_{c,c}(\tau)$ using parameters that correspond to the three previously shown stochastic trajectories (Fig. 4 *Aa–c*). In the absence of buffer, $\phi_{c,c}(\tau)$ decays by 50% when $\tau \approx 5$ ms, consistent with the time constant for

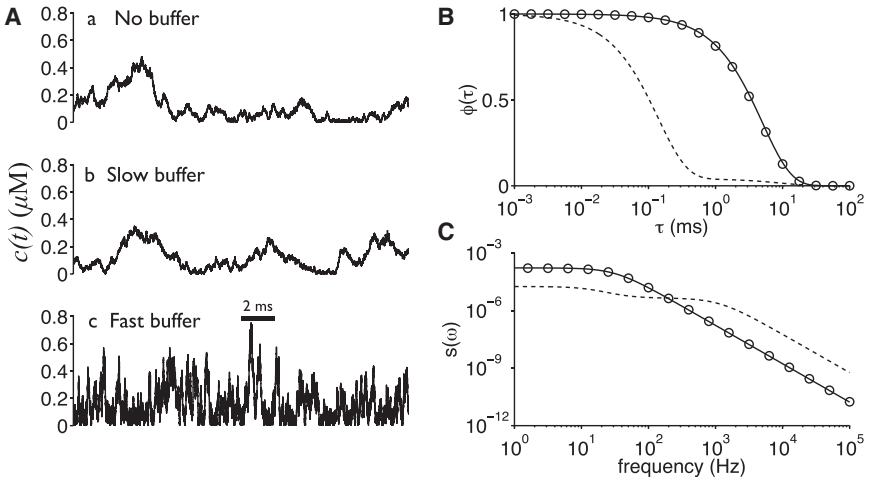

FIGURE 4 Influence of buffer on the time evolution of $[Ca^{2+}]$ fluctuations. (*A*) Monte Carlo simulation of domain $[Ca^{2+}]$, $c(t)$, for different buffer parameters. (*B*) Autocorrelation function ($\phi_{c,c}$ (τ), Eq. 45) and (*C*) power spectrum ($s_{c,c}(\omega)$, Eq. 46) in the presence of slow (*open circles*) and fast (*dashed line*) buffer and in the absence of buffer (*solid line*). Autocorrelation function curves are normalized by the steady-state variance such that $\phi_{c,c}$ (0) = 1. Parameters: c_{ss} = 0.1 μM, c_∞ = 0.1 μM, k_c = 0.2 ms^{-1}, and $\Omega = 10^{-17}$ *L*. Buffer parameters: b_T^∞ μM, κ = 0.2 μM, $k_b = 10^{-1}$ ms^{-1}, $k_+ = 10^{-3}$ (slow), and 1 (fast) μM^{-1} ms^{-1}.

Ca^{2+} exchange (k_c = 0.2 ms^{-1}, *solid line*). In the presence of slow buffer, $\phi_{c,c}(\tau)$ is nearly identical (*open circles*), but in the presence of fast buffer the 50% decay occurs at a much shorter time ($\tau \approx$ 0.1 ms, *dashed line*).

The time evolution of the domain $[Ca^{2+}]$ fluctuation $\delta c(t)$ can also be characterized by its (colored) power spectrum, that is, the 3×3 matrix $S(\omega) = (s_{i,j})$,

$$S(\omega) = (i\omega I + H_{ss})^{-1}\,\Gamma_{ss}\left(-i\omega I + H_{ss}^T\right)^{-1} \qquad (46)$$

that reduces to

$$s_{c,c}^0(\omega) = 2k_c c_{ss}\Big/\left[\Omega\left(\omega^2 + k_c^2\right)\right]$$

in the absence of buffer (26). Fig. 4 *C* shows the power spectrum $s_{c,c}(\omega)$ in the absence of buffer and in the presence of slow buffer (*solid line*, *open circles*). In both cases, the spectrum is low-pass, but for fast buffer, $s_{c,c}(\omega)$ drops off at higher frequency (smaller τ, *dashed line*), consistent with the higher frequency fluctuations observed in Fig. 4 *A*. In addition to clarifying the frequency content of domain $[Ca^{2+}]$ fluctuations, this power spectrum analysis illustrates how buffers influence fluctuations even in the absence of Ca^{2+} influx. Further analysis of the influence of buffers on the timescale of domain $[Ca^{2+}]$ fluctuations is provided in Fig. S4 and Fig. S5.

DISCUSSION

Relation to prior work

The influence of Ca^{2+} buffers on Ca^{2+} diffusion, oscillations, propagating Ca^{2+} waves, and spatially localized Ca^{2+} elevations has received considerable attention in recent years (for reviews focused on local signaling, see Berridge (2,43), Smith et al. (45), and Augustine et al. (46)). Previous studies have presented theoretical analysis of buffered Ca^{2+} diffusion and localized Ca^{2+} elevations (16–18,20,47–49), as well as stochastic aspects of Ca^{2+}-induced Ca^{2+} release, Ca^{2+} oscillations, and propagating Ca^{2+} waves (34,50–53). A subset of these studies utilized a Langevin formulation for the dynamics of intracellular Ca^{2+} channels (54–56).

Models of Ca^{2+}-regulated Ca^{2+} channels and stochastic Ca^{2+} release usually incorporate buffering into the domain description and, more rarely, consider the fluctuations in free $[Ca^{2+}]$ that result from the small volume of subcellular compartments (e.g., the cardiac dyadic subspace) (30,33–35). To our knowledge, this is the first study that formulates Langevin equations for the buffered dynamics of intracellular Ca^{2+} and, subsequently, characterizes the influence of Ca^{2+} buffers on $[Ca^{2+}]$ fluctuations that arise from the association and dissociation of Ca^{2+} and buffer. The analytical results pertaining to the fluctuating rapid buffer approximation (RBA) and the influence of buffers' properties on fluctuation amplitude is, to our knowledge, entirely novel.

Previous studies have, of course, utilized Langevin equations to simulate concentration fluctuations in other biochemical systems (30,33,57–60) and the stochastic gating of plasma membrane and intercellular ion channels (54,55,61–64), and used the fluctuation-dissipation theorem to characterize concentration fluctuations in biochemical reaction networks, e.g., in models of gene networks and Michaelis-Menten enzyme reactions (65–68). However, to our knowledge, this is the first mathematical analysis of domain $[Ca^{2+}]$ fluctuations in the presence of Ca^{2+} buffers.

Summary of findings

The fluctuating RBA derived above shows how the Ca^{2+} and buffer exchange rates (k_c and k_b), total buffer concentration (b_T^∞), and dissociation constant (κ) influence $[Ca^{2+}]$ fluctuations. Typically, fast buffer binding and high exchange rates increase the size of $[Ca^{2+}]$ fluctuations ($\sigma_c^{ss} = \langle \delta c^2 \rangle$). The fluctuating RBA derived here shows that the relative increase in fluctuation size due to buffers, i.e., the ratio of

coefficients of variation (Eq. 40), is an increasing function of the steady-state domain $[Ca^{2+}]$ (c_{ss}) and thus an increasing function of Ca^{2+} influx rate (j_{in}). For fixed steady-state domain $[Ca^{2+}]$, $c_{ss} > c_\infty$, Fig. 2 and Eq. 40 show that the relative fluctuation size c_v'/c_v^0 is a biphasic function of the total buffer concentration b_T^∞. At low b_T^∞, the fluctuation amplitude approaches that observed in the absence of buffer ($c_v' \approx c_v^0$, $w_{ss} \to 0$ in Eq. 37). At high b_T^∞, the ratio $c_v'/c_v^0 \approx 1$ because increased buffering capacity attenuates the buffer-mediated increase in free $[Ca^{2+}]$ fluctuations ($\beta_{ss} \to 0$ in Eq. 37). The total buffer concentration that maximizes c_v'/c_v^0 is given by Eq. 42. For a fixed Ca^{2+} influx rate j_{in}, c_{ss} is a decreasing sigmoidal function of b_T^∞ that approaches c_∞ (Eq. 20). In this case, σ_c^{ss} is a decreasing sigmoidal function that approaches c_∞/Ω. However, the buffer-mediated change in fluctuation size as measured by

$$c_v'\Big/c_v^0 = \sqrt{1+\chi} \geq 1,$$

remains a biphasic function of b_T^∞. For fixed c_{ss} and for fixed j_{in}, Ca^{2+} buffers increase the amplitude of domain $[Ca^{2+}]$ fluctuation.

We explore the validity of the RBA for realistic buffer parameters and microdomain geometries and find the fluctuating RBA is a good approximation when buffer kinetics are rapid compared to the Ca^{2+} and buffer exchange rates. Exchange rates on domain volume depends on the presumed relationship between escape target size and linear dimension of the domain. However, the fluctuating RBA agrees with the full calculation whenever the physical domain volume is sufficiently large and/or the escape passage is sufficiently narrow, because both situations lead to exchange rate constants (k_c and k_b) that are small compared to the buffer equilibration rate (an increasing function of both k_+ and k_-). As one would expect based on these considerations, the fluctuating RBA is a better approximation to the full equations for domain $[Ca^{2+}]$ fluctuations for mushroom-shaped (as opposed to thin or stubby) dendritic spine geometries (Fig. 3 *D*).

Our analysis shows that a buffer-mediated increase in intrinsic $[Ca^{2+}]$ fluctuations requires a nonequilibrium steady state, that is, a gradient between domain and bulk Ca^{2+} ($c_{ss} > c_\infty$), which implies disequilibrium between Ca^{2+} and buffer within the domain. However, our primary result that buffers do not suppress intrinsic $[Ca^{2+}]$ fluctuations—due to the buffer's contribution to these fluctuations—is true in the absence, as well as the presence, of elevated domain $[Ca^{2+}]$. Although buffers do not influence the steady-state variance of domain $[Ca^{2+}]$ fluctuations in the absence of Ca^{2+} influx, power spectrum analysis shows that buffers do alter the temporal dynamics of domain $[Ca^{2+}]$ fluctuations. For fixed $\kappa = k_-/k_+$, a faster association rate constant (k_+) leads to higher frequency free $[Ca^{2+}]$ fluctuations and shorter autocorrelation times.

Buffers suppress extrinsic (not intrinsic) domain $[Ca^{2+}]$ fluctuations

As discussed in the Introduction, the effective volume that arises in the deterministic equations for the buffered diffusion of intracellular Ca^{2+} is

$$\Omega_{\text{eff}} = \Omega/\beta(c),$$

where $\Omega_{\text{eff}} \geq \Omega$ because $0 < \beta(c) \leq 1$ (24). Because the relative size of concentration fluctuations decreases as system size increases, one might expect that domain $[Ca^{2+}]$ fluctuations would decrease as total buffer concentration increases. In marked contrast to this conjecture, the analysis of domain $[Ca^{2+}]$ fluctuations presented here demonstrates that buffers increase the size of $[Ca^{2+}]$ fluctuations (during periods of Ca^{2+} influx) or have no influence (when there is no influx). That is, buffers typically lead to domain $[Ca^{2+}]$ fluctuations with variance σ_c^{ss} that is consistent with a domain that lacks buffers but has smaller physical volume.

Some clarity with regard to this counterintuitive result can be obtained by revisiting the fast/slow system of stochastic ODEs for buffered Ca^{2+} dynamics (Eq. 34) under the restriction that Ca^{2+}-free or Ca^{2+}-bound buffer do not exchange with bulk ($k_b = 0$),

$$\dot{\delta c} = -[k_+(c_{ss}+b_{ss})+k_- + k_c]\delta c + (k_+c_{ss} + k_-)\delta c_T + \xi_c^{ss}(t), \tag{47a}$$

$$\dot{\delta c}_T = -k_c\delta c + \xi_{c_T}^{ss}(t). \tag{47b}$$

Here the fluctuation is free $[Ca^{2+}]$. The value (δc) is the fast variable and δc_T is the only slow variable because the domain total buffer concentration is a conserved quantity given by initial conditions ($b_T = b(0) + cb(0)$) and does not fluctuate ($\delta b_T = 0$). Setting $k_b = 0$ in Eq. 37, we see that under this restriction $\chi = 0$, and the fluctuating RBA result is identical to the case without buffers,

$$c_v' = c_v^0 = 1\Big/\sqrt{c_{ss}\Omega},$$

because immobile buffers ($k_b = 0$) do not change the steady-state variance of domain $[Ca^{2+}]$ fluctuations. Note that when $k_b = 0$, the differential fraction of free to total calcium (β_{ss}) appears in the quasistatic approximation,

$$\langle \delta c \rangle_* \approx \beta_{ss}\delta c_T$$

and the slow equation,

$$\dot{\delta c}_T = -\beta_{ss}k_c\delta c_T + \xi_{c_T}^{ss}(t), \tag{48}$$

precisely as one would expect. Using the fluctuation-dissipation equation (Eq. 30), we calculate the steady-state covariance of the total calcium concentration,

$$\langle \delta c_T^2 \rangle = \frac{\gamma_c^{ss}}{2\beta_{ss}k_c} = \frac{2k_c c_{ss}}{2\beta_{ss}k_c\Omega} = \frac{c_{ss}}{\beta_{ss}\Omega}, \tag{49}$$

as well as the covariances that involve the fast variable δc. In the RBA limit with $k_b = 0$, the latter are given by

$$\langle \delta c\ \delta c_T \rangle = \beta_{ss}\langle \delta c_T^2 \rangle = \frac{c_{ss}}{\Omega} \tag{50a}$$

and

$$\langle \delta c^2 \rangle = \frac{\gamma_r^{ss}}{2[k_+(c_{ss}+b_{ss})+k_-]} + \beta_{ss}^2\langle \delta c_T^2 \rangle \tag{50b}$$

$$= (1-\beta_{ss})\frac{c_{ss}}{\Omega} + \beta_{ss}\frac{c_{ss}}{\Omega} = \frac{c_{ss}}{\Omega}, \tag{50c}$$

where for the second equality we have used $\beta_{ss}w_{ss} = 1-\beta_{ss}$ and the definition of γ_r^{ss} (Eq. 23).

Equation 49 shows that the covariance of the total $[Ca^{2+}]$ fluctuation ($\langle \delta c_T^2 \rangle$) responds to the elementary processes of Ca^{2+} influx and exchange with the bulk

$$\gamma_c^{ss} = [j_{in} + k_c(c_{ss}+c_\infty)]/\Omega = 2k_c c_{ss}/\Omega.$$

The covariance of the free $[Ca^{2+}]$ is also dependent on influx and exchange (γ_c^{ss}) through the term $\beta_{ss}^2\langle \delta c_T^2 \rangle$. The value $\langle \delta c^2 \rangle$ is influenced by the elementary processes of Ca^{2+} and buffer association and dissociation

$$\gamma_r^{ss} = [k_+ c_{ss}b_{ss} + k_- c b_{ss}]/\Omega,$$

whereas $\langle \delta c_T^2 \rangle$ is not. Increasing buffer concentration (b_T^∞) decreases β_{ss} and increases $\langle \delta c_T^2 \rangle$. The value b_T^∞ also scales γ_r^{ss} in such a way that $\langle \delta c^2 \rangle$ is unchanged. Stationary buffers do not influence the steady-state covariance of domain $[Ca^{2+}]$ fluctuations ($k_b = 0$), because the intrinsic nature of the fluctuating force $\xi_c^{ss}(t)$ causes γ_r^{ss} and β_{ss} to be related in a manner that makes $\langle \delta c^2 \rangle = c_{ss}/\Omega$ invariant to the buffer parameter b_T^∞ and κ.

However, if the influx rate were modulated so that there was an extrinsic component to the fluctuations,

$$j_{in}(t) = j_{in}^0 + j_{in}^1(t)$$

where

$$j_{in}^0 = k_c(c_{ss}-c_\infty) \text{ and } \langle j_{in}^1(t)\, j_{in}^1(t')\rangle = \gamma_{in}^{ss}\delta(t-t'),$$

where $\gamma_{in}^{ss} = j_{ext}^{ss}/\Omega$, then the fluctuating terms in both Eqs. 47a and 47b would have greater variance and Eqs. 49 and 50b become

$$\langle \delta c_T^2 \rangle = \frac{\gamma_c^{ss}+\gamma_{in}^{ss}}{2\beta_{ss}k_c} = \frac{c_{ss}}{\beta_{ss}\Omega}\left(1+\frac{j_{ext}^{ss}}{2k_c c_{ss}}\right)$$

and

$$\langle \delta c^2 \rangle = \frac{\gamma_r^{ss}+\gamma_{in}^{ss}}{2[k_+(c_{ss}+b_{ss})+k_-]} + \beta_{ss}^2\langle \delta c_T^2 \rangle$$

$$= (1-\beta_{ss})\frac{c_{ss}}{\Omega} + \beta_{ss}\frac{c_{ss}}{\Omega}\left(1+\frac{j_{ext}^{ss}}{2k_c c_{ss}}\right) = \frac{c_{ss}}{\Omega}\left(1+\beta_{ss}\frac{j_{ext}^{ss}}{2k_c c_{ss}}\right),$$

where we have used the fact that $\gamma_{in}^{ss}/k_+ \to 0$ in the RBA limit. From the last equality we conclude that the variance of the external drive γ_{in}^{ss} increases the steady-state variance of domain $[Ca^{2+}]$ fluctuations. The location of the coefficient β_{ss} in the term $(1+\beta_{ss}j_{ext}^{ss}/2k_c c_{ss})$ shows that stationary buffers are able to suppress such extrinsic variability of Ca^{2+} influx/efflux rate, despite the fact that the buffers do not suppress intrinsic fluctuations (compare to Eq. 50b).

Analysis of the fluctuating RBA and intrinsic fluctuations

Analysis of the fluctuating RBA also provides insight into intrinsic (buffer-driven) fluctuations when both Ca^{2+} and buffer exchange with bulk ($k_b \neq 0$). The quasistatic approximation for the average value of the $[Ca^{2+}]$ fluctuation in the fluctuating RBA (Eq. 35) shows that the free (δc) and total (δc_T) calcium fluctuations are related by the factor β_{ss} as expected. Also, Eq. 36a shows that total buffer concentration b_T^∞ slows the relaxation of total calcium fluctuations (δc_T) through the factor β_{ss}. However, the relaxation of total buffer (δb_T) fluctuations are not slowed in this manner (Eq. 36b) and, importantly, the entries of the covariance matrix for the random terms ξ_c^{ss}, $\xi_{c_T}^{ss}$, and $\xi_{b_T}^{ss}$, are all proportional to the total buffer concentration b_T^∞ (Eq. S18 and Eq. S20 in the Supporting Material).

To understand the interplay between the effect of b_T^∞ on the random terms (fluctuation) and the relaxation rate (dissipation) in the case of mobile buffers ($k_b > 0$), we analyze the Langevin domain model when the exchange rates for Ca^{2+} and buffer are identical ($k_c = k_b = k$). Under this restriction, the covariances of the slow variables are given by

$$\langle \delta c_T^2 \rangle = \frac{c_{ss}+cb_{ss}}{\Omega},$$
$$\langle \delta c_T\ \delta b_T \rangle = \frac{cb_{ss}+cb_\infty}{2\Omega}, \tag{51}$$
$$\langle \delta b_T^2 \rangle = \frac{b_T^\infty}{\Omega},$$

where the $c_{ss}+cb_{ss}$ value in the numerator of $\langle \delta c_T^2 \rangle$ is the steady-state total calcium concentration in the domain. The variance of the fast variable $\langle \delta c^2 \rangle$ can be written in terms of the covariances of the slow variables,

$$\langle \delta c^2 \rangle = \beta_{ss}\left[w_{ss}\frac{c_{ss}}{\Omega} + \beta_{ss}\left(\langle \delta c_T^2 \rangle - 2\nu_{ss}\langle \delta c_T\, \delta b_T \rangle + \nu_{ss}^2 \langle \delta b_T^2 \rangle\right)\right], \tag{52}$$

and it can be shown that $\langle \delta c \delta b_T \rangle$ is negative whereas $\langle \delta c \delta c_T \rangle$ and $\langle \delta c^2 \rangle$ are positive. Upon substitution of Eq. 51, we have

$$\langle \delta c^2 \rangle = \frac{\beta_{ss}}{\Omega}\left\{w_{ss}c_{ss} + \beta_{ss}\left[c_{ss} + cb_{ss} - \nu_{ss}(cb_{ss} + cb_\infty) + \nu_{ss}^2 b_T^\infty\right]\right\}, \tag{53a}$$

$$= \frac{1}{\Omega}\left\{(1-\beta_{ss})c_{ss} + \beta_{ss}^2\left[c_{ss} + cb_{ss} - \nu_{ss}(cb_{ss} + cb_\infty) + \nu_{ss}^2 b_T^\infty\right]\right\}. \tag{53b}$$

In this case, the fluctuating RBA simplifies to

$$\sigma_c' = \frac{c_{ss}}{\Omega} \times (1+\chi), \qquad \chi = \frac{w_{ss}}{(1+w_{ss})^2} \times \frac{c_{ss} - c_\infty}{\kappa + c_\infty}. \tag{54}$$

This analysis of the fluctuating RBA under the restriction $k_c = k_b$ shows that an increase in total buffer b_T^∞ increases the absolute value of the slow covariances (Eq. 51). These covariances (the terms within square brackets in Eq. 53) combine to create a net positive impact on $\langle \delta c^2 \rangle$ that is attenuated to some extent by a decrease in the β_{ss} that scales these terms. The β_{ss}/Ω value outside the curly brackets in Eq. 53a might be interpreted as an effective volume that attenuates all of these contributions to $\langle \delta c^2 \rangle$, but this is misleading because $\beta_{ss}w_{ss}c_{ss} = (1 - \beta_{ss})c_{ss}$ is an increasing function of b_T^∞ (compare to Eq. 53b). Furthermore, Eq. 54 shows that the variance of the free $[Ca^{2+}]$ fluctuations in the presence of buffer $b_T^\infty > 0$ is never less than what would occur in the absence of buffer ($b_T^\infty = 0$).

All of the expressions in this section have counterparts when the fluctuating RBA is derived in full generality ($k_c \neq k_b$, see Appendix B in the Supporting Material). The derivation of the fluctuating RBA when $k_c = k_b$ is shown in Appendix C in the Supporting Material.

Physiological implications

Ca^{2+} is an important signaling molecule in many cell types. Intracellular Ca^{2+} regulates cellular responses through Ca^{2+}-regulated ion channels, Ca^{2+}-dependent kinases, and phosphotases, and key processes in excitable cells, including muscle contraction and neurotransmitter release (1). Many of these signaling pathways occur in small spatially restricted volumes (microdomains) and, consequently, fluctuations in $[Ca^{2+}]$ may be physiologically significant. Our results are broadly applicable to subcellular Ca^{2+} domains, including dendritic spines, the dyadic cleft, and many other situations where localized Ca^{2+} elevations occur in spatially restricted subcellular compartments, such as the primary cilium, mitochondria-ER junctions, and endoplasmic reticulum/plasma membrane (ER/PM) junctional regions (Fig. 1). As a concrete example of an application of the theory, we found—using physiological values for dendritic spine shape—that the exogenous Ca^{2+} buffer BAPTA does not suppress intrinsic domain $[Ca^{2+}]$ fluctuations, and may increase the coefficient of variation (c_v) of domain $[Ca^{2+}]$ fluctuations by a factor of 2 or more (Fig. 3 *D*).

Spatially localized subcellular dynamics can greatly alter whole-cell or even tissue-level physiological processes. For example, in the cardiac dyadic subspace, the regenerative (i.e., positive feedback) nature of Ca^{2+}-induced Ca^{2+}-release creates a subcellular environment where the spontaneous opening of only a few Ca^{2+} channels can lead to opening of nearly all of the channels in a dyad (essentially an all-or-none response) (69). Ca^{2+} release that spontaneously initiates within one dyad may activate neighboring dyads resulting in propagating Ca^{2+} waves. In pathophysiological conditions this may lead to ectopic heart beats that are potentially arrhythmogenic. This is one of many examples where the spatially localized stochastic dynamics of a few Ca^{2+} channels may influence the global Ca^{2+} response and, for this reason, the regulation of Ca^{2+} channels by buffer-modulated $[Ca^{2+}]$ fluctuations may be physiologically significant.

In Weinberg and Smith (35), we developed and analyzed a minimal model of a Ca^{2+} microdomain that included a stochastically gating Ca^{2+}-regulated Ca^{2+} channel and accounted for the small number of Ca^{2+} ions present in the domain at any given time. This prior work demonstrated that $[Ca^{2+}]$ fluctuations due to small domain volumes could alter the open probability of Ca^{2+} channels, typically reducing the open probability compared with larger volumes. The fluctuating RBA derived here shows that Ca^{2+} buffers typically enhance domain $[Ca^{2+}]$ fluctuations and, when combined with previous work, this suggests that buffers may influence the stochastic dynamics of Ca^{2+}-regulated Ca^{2+} channels (the frequency and duration of channel openings) and potentially influence the stochastic properties of local Ca^{2+} release events (sparks and puffs).

Our analysis of the fluctuating RBA raises the intriguing question of whether or not domain $[Ca^{2+}]$ fluctuations are physiologically significant aspects of local (and perhaps global) Ca^{2+} signaling. This topic requires further study, in part because our mathematical analysis indicates that Ca^{2+} chelators and indictor dyes enhance intrinsic domain $[Ca^{2+}]$ fluctuations. The physiological relevance of domain $[Ca^{2+}]$ fluctuations on the dynamics of signaling complexes will presumably depend on the timescale of Ca^{2+} influx, the geometry of the microdomain, and the kinetics of downstream Ca^{2+}-dependent signaling.

Limitations of this analysis

We have shown that $[Ca^{2+}]$ fluctuations in spatially restricted subcellular compartments cannot be suppressed by increasing the total concentration of Ca^{2+} buffer (b_T^∞). Of course, this conclusion that Ca^{2+} buffers typically enhance domain $[Ca^{2+}]$ fluctuations pertains only to buffers whose dynamics are well represented by the bimolecular association reaction that was our starting point (Eq. 1). It is possible that Ca^{2+} buffers with more complicated and realistic Ca^{2+}-binding kinetics (e.g., cooperative binding) may suppress free $[Ca^{2+}]$ fluctuations. This question could be addressed rigorously using chemical reaction network theory.

Although we consider Ca^{2+} and buffer transport via exchange between domain and bulk, this work does not use continuum modeling (partial differential equations) to explicitly represent spatial aspects of the buffered diffusion of intracellular Ca^{2+}. Spatial correlations in fluctuations are of interest, but beyond the scope of this study, in part because the mathematical description of diffusion-mediated concentration fluctuations is less accessible than the analysis of stochastic differential equations presented here.

This article has focused on intrinsic Ca^{2+} and buffer concentration fluctuations around nonequilibrium steady states in the presence of Ca^{2+} influx ($j_{in} > 0$) and equilibrium steady states in the absence of Ca^{2+} influx ($j_{in} = 0$). Our analytical work is relevant and easily applied whenever a separation of timescales exists between the concentration fluctuations per se (that arise from finite size effects) and temporal variations in Ca^{2+} influx rate. For example, during the cardiac cycle, triggered release of junctional sarcoplasmic reticulum (SR) Ca^{2+} elevates dyadic subspace $[Ca^{2+}]$ for durations of ~300 ms, and the low $[Ca^{2+}]$ of the diastolic interval persists for ~500 ms. Because domain $[Ca^{2+}]$ fluctuations occur on a faster timescale (1–10 ms), it is straightforward to apply our theory to the cardiac dyad under the assumption that domain concentrations (expected values) are in quasistatic equilibrium with the time-varying influx rate, i.e., $c_{ss}(t) = c_{ss}(j_{in}(t))$ through Eq. 20 and similarly for $b_{ss}(t)$ and $cb_{ss}(t)$. Even when no such timescale separation exists, domain $[Ca^{2+}]$ fluctuations in the context of time-varying Ca^{2+} influx can be calculated by numerical integration of Eq. 27, with $H_{ss}(t)$ and $\Gamma_{ss}(t)$ evaluated at the time-varying expected values of the domain Ca^{2+} and buffer concentrations (26). Such quasistatic and nonstationary calculations agree with numerical simulations of domain $[Ca^{2+}]$ fluctuations during triggered release (see Fig. S6). Perhaps most importantly, such calculations confirm that buffers increase intrinsic domain $[Ca^{2+}]$ fluctuations during systole, and buffers do not suppress $[Ca^{2+}]$ fluctuations during diastole, just as one would expect from the nonequilibrium steady-state analysis that has been our focus.

In other physiological settings, domain $[Ca^{2+}]$ is elevated for longer or shorter durations. In pancreatic β-cells, for example, insulin secretion is regulated by minute-long duration $[Ca^{2+}]$ elevations in nuclear (8) and subplasma membrane (70) Ca^{2+} microdomains. In pituitary cells, minute-long spontaneous $[Ca^{2+}]$ oscillations have been observed in mitochondrial microdomains (71). In such cases, it is straightforward to apply our nonequilibrium steady-state analysis (e.g., the fluctuating RBA). This article's conclusions are also directly applicable to the case of pulsatile Ca^{2+} influx with characteristic time shorter than the domain equilibration time (for buffers and escape). When the timescale for pulsatile influx is comparable to the domain time constant, quantitative studies will require simulation of the full system of stochastic ODEs. In numerical simulation of a stochastically gated influx with mean open time of 1 ms and mean closed time of 9 ms, we find that buffers do not decrease intrinsic domain $[Ca^{2+}]$ fluctuations (see Fig. S7), consistent with our analysis of constant and slowly changing Ca^{2+} influx.

It would be interesting to understand the impact of intrinsic fluctuations (due to the finite number of Ca^{2+} ions in a domain) on Ca^{2+}-mediated effectors, including Ca^{2+}-activated or inactivated channels, initiation of Ca^{2+} sparks, and so on. In complementary projects we have made some progress in that direction (35). It is important to understand that even when $[Ca^{2+}]$ fluctuations are much faster than the timescale of a downstream Ca^{2+}-mediated process (e.g., opening of a Ca^{2+}-activated channel), these fluctuations may (34) or may not (35) average-out over the slower timescale. Further studies could address such issues by including downstream signaling events in model formulations, but this article's primary conclusion—that Ca^{2+} buffers do not suppress intrinsic $[Ca^{2+}]$ fluctuations—is an important first step in our developing understanding of the physiological significance of domain $[Ca^{2+}]$ fluctuations.

SUPPORTING MATERIAL

Supporting Results, with Validation of the Linear Noise Approximation, $[Ca^{2+}]$ Fluctuations in the Presence of Multiple Buffers, Influence of the Buffer Dissociation Constant κ on $[Ca^{2+}]$ Fluctuations, Timescale of Domain $[Ca^{2+}]$ Fluctuations, $[Ca^{2+}]$ Fluctuations during a Time-Varying Ca^{2+} Influx, Appendix A: The Chemical Langevin Equation and Linear Noise Approximation, Appendix B: Derivation of the Rapid Buffer Approximation, Appendix C: Analysis of the Fluctuating RBA and Intrinsic Fluctuations, and seven figures are available at http://www.biophysj.org/biophysj/supplemental/S0006-3495(14)00464-0.

The authors thank the referees for helpful and constructive comments.

The work was supported by National Science Foundation grant No. DMS 1121606, the Biomathematics Initiative at The College of William & Mary, and a 2013 Plumeri Award for Faculty Excellence to G.D.S.

REFERENCES

1. Berridge, M. J., M. D. Bootman, and H. L. Roderick. 2003. Calcium signaling: dynamics, homeostasis and remodeling. *Nat. Rev. Mol. Cell Biol.* 4:517–529.

2. Berridge, M. J. 1998. Neuronal calcium signaling. *Neuron.* 21:13–26.
3. Berridge, M. J. 2006. Calcium microdomains: organization and function. *Cell Calcium.* 40:405–412.
4. Carrasco, M. A., and C. Hidalgo. 2006. Calcium microdomains and gene expression in neurons and skeletal muscle cells. *Cell Calcium.* 40:575–583.
5. Demuro, A., and I. Parker. 2006. Imaging single-channel calcium microdomains. *Cell Calcium.* 40:413–422.
6. Koh, X., B. Srinivasan, …, A. Levchenko. 2006. A 3D Monte Carlo analysis of the role of dyadic space geometry in spark generation. *Biophys. J.* 90:1999–2014.
7. Winslow, R. L., and J. L. Greenstein. 2011. Cardiac myocytes and local signaling in nano-domains. *Prog. Biophys. Mol. Biol.* 107:48–59.
8. Alonso, M. T., C. Villalobos, …, J. García-Sancho. 2006. Calcium microdomains in mitochondria and nucleus. *Cell Calcium.* 40:513–525.
9. Dedkova, E. N., and L. A. Blatter. 2013. Calcium signaling in cardiac mitochondria. *J. Mol. Cell. Cardiol.* 58:125–133.
10. Kohlhaas, M., and C. Maack. 2013. Calcium release microdomains and mitochondria. *Cardiovasc. Res.* 98:259–268.
11. Lindemann, B. 2001. Predicted profiles of ion concentrations in olfactory cilia in the steady state. *Biophys. J.* 80:1712–1721.
12. Pazour, G. J., and G. B. Witman. 2003. The vertebrate primary cilium is a sensory organelle. *Curr. Opin. Cell Biol.* 15:105–110.
13. Delling, M., P. G. DeCaen, …, D. E. Clapham. 2013. Primary cilia are specialized calcium signaling organelles. *Nature.* 504:311–314.
14. Smith, G. D. 2001. Modeling local and global calcium signals using reaction diffusion equations. *In* Computational Neuroscience. CRC Press, Boca Raton, FL.
15. Smith, G. D., J. Wagner, and J. Keizer. 1996. Validity of the rapid buffering approximation near a point source of calcium ions. *Biophys. J.* 70:2527–2539.
16. Smith, G. D. 1996. Analytical steady-state solution to the rapid buffering approximation near an open Ca^{2+} channel. *Biophys. J.* 71:3064–3072.
17. Smith, G. D., L. Dai, …, A. Sherman. 2001. Asymptotic analysis of buffered calcium diffusion near a point source. *SIAM J. Appl. Math.* 61:1816–1838.
18. Naraghi, M., and E. Neher. 1997. Linearized buffered Ca^{2+} diffusion in microdomains and its implications for calculation of $[Ca^{2+}]$ at the mouth of a calcium channel. *J. Neurosci.* 17:6961–6973.
19. Shuai, J., J. E. Pearson, and I. Parker. 2008. Modeling Ca^{2+} feedback on a single inositol 1,4,5-trisphosphate receptor and its modulation by Ca^{2+} buffers. *Biophys. J.* 95:3738–3752.
20. Stern, M. D. 1992. Buffering of calcium in the vicinity of a channel pore. *Cell Calcium.* 13:183–192.
21. Dargan, S. L., and I. Parker. 2003. Buffer kinetics shape the spatiotemporal patterns of IP_3-evoked Ca^{2+} signals. *J. Physiol.* 553:775–788.
22. Zeller, S., S. Rüdiger, …, M. Falcke. 2009. Modeling of the modulation by buffers of Ca^{2+} release through clusters of IP_3 receptors. *Biophys. J.* 97:992–1002.
23. Tsai, J.-C., and J. Sneyd. 2011. Traveling waves in the buffered Fitz-Hugh-Nagumo model. *SIAM J. Appl. Math.* 71:1606–1636.
24. Wagner, J., and J. Keizer. 1994. Effects of rapid buffers on Ca^{2+} diffusion and Ca^{2+} oscillations. *Biophys. J.* 67:447–456.
25. van Kampen, N. G. 1981. Stochastic Processes in Physics and Chemistry. North-Holland Publishing Company, Amsterdam, The Netherlands.
26. Keizer, J. 1987. Statistical Thermodynamics of Nonequilibrium Processes. Springer, Berlin, Germany.
27. Rüdiger, S., J. W. Shuai, …, M. Falcke. 2007. Hybrid stochastic and deterministic simulations of calcium blips. *Biophys. J.* 93:1847–1857.
28. Huertas, M. A., and G. D. Smith. 2007. The dynamics of luminal depletion and the stochastic gating of Ca^{2+}-activated Ca^{2+} channels and release sites. *J. Theor. Biol.* 246:332–354.
29. Groff, J. R., and G. D. Smith. 2008. Calcium-dependent inactivation and the dynamics of calcium puffs and sparks. *J. Theor. Biol.* 253:483–499.
30. von Wegner, F., and R. H. A. Fink. 2010. Stochastic simulation of calcium microdomains in the vicinity of an L-type calcium channel. *Eur. Biophys. J.* 39:1079–1088.
31. Williams, G. S. B., A. C. Chikando, …, M. S. Jafri. 2011. Dynamics of calcium sparks and calcium leak in the heart. *Biophys. J.* 101:1287–1296.
32. Rüdiger, S., P. Jung, and J.-W. Shuai. 2012. Termination of Ca^{2+} release for clustered IP_3R channels. *PLOS Comput. Biol.* 8:e1002485.
33. Winslow, R. L., A. Tanskanen, …, J. L. Greenstein. 2006. Multiscale modeling of calcium signaling in the cardiac dyad. *Ann. N. Y. Acad. Sci.* 1080:362–375.
34. Hake, J., and G. T. Lines. 2008. Stochastic binding of Ca^{2+} ions in the dyadic cleft; continuous versus random walk description of diffusion. *Biophys. J.* 94:4184–4201.
35. Weinberg, S. H., and G. D. Smith. 2012. Discrete-state stochastic models of calcium-regulated calcium influx and subspace dynamics are not well-approximated by ODEs that neglect concentration fluctuations. *Comput. Math. Methods Med.* 2012:897371.
36. Schuss, Z., A. Singer, and D. Holcman. 2007. The narrow escape problem for diffusion in cellular microdomains. *Proc. Natl. Acad. Sci. USA.* 104:16098–16103.
37. Gillespie, D. T. 2000. The chemical Langevin equation. *J. Chem. Phys.* 113:297–306.
38. Higham, D. J. 2008. Modeling and simulating chemical reactions. *SIAM Rev.* 50:347–368.
39. Gardiner, C. W. 1997. Handbook of Stochastic Methods for Physics, Chemistry, and the Natural Sciences. Springer, New York.
40. Gillespie, D. T. 2007. Stochastic simulation of chemical kinetics. *Annu. Rev. Phys. Chem.* 58:35–55.
41. Harris, K. M., F. E. Jensen, and B. Tsao. 1992. Three-dimensional structure of dendritic spines and synapses in rat hippocampus (CA_1) at postnatal day 15 and adult ages: implications for the maturation of synaptic physiology and long-term potentiation. *J. Neurosci.* 12:2685–2705.
42. Laub, A. J. 2004. Kronecker products. *In* Matrix Analysis for Scientists and Engineers Society for Industrial and Applied Mathematics (SIAM), Philadelphia, PA.
43. Berridge, M. J. 1997. Elementary and global aspects of calcium signaling. *J. Physiol.* 499:291–306.
44. Reference deleted in proof.
45. Smith, G. D., J. Pearson, and J. Keizer. 2002. Modeling intracellular Ca^{2+} waves and sparks. *In* Computational Cell Biology. C. Fall, E. Marland, J. Wagner, and J. Tyson, editors. Springer, Berlin, Germany, pp. 200–232.
46. Augustine, G. J., F. Santamaria, and K. Tanaka. 2003. Local calcium signaling in neurons. *Neuron.* 40:331–346.
47. Neher, E. 1986. Concentration profiles of intracellular Ca^{2+} in the presence of diffusible chelator. *Exp. Brain Res.* 14:80–96.
48. Reference deleted in proof.
49. Falcke, M. 2003. Buffers and oscillations in intracellular Ca^{2+} dynamics. *Biophys. J.* 84:28–41.
50. Shuai, J. W., and P. Jung. 2003. Langevin modeling of intracellular calcium dynamics. *In* Understanding Calcium Dynamics Springer, Berlin, Germany, pp. 231–252.
51. Nguyen, V., R. Mathias, and G. D. Smith. 2005. A stochastic automata network descriptor for Markov chain models of instantaneously coupled intracellular Ca^{2+} channels. *Bull. Math. Biol.* 67:393–432.
52. Jafri, M. S., and J. Keizer. 1995. On the roles of Ca^{2+} diffusion, Ca^{2+} buffers, and the endoplasmic reticulum in IP_3-induced Ca^{2+} waves. *Biophys. J.* 69:2139–2153.
53. Thul, R., and M. Falcke. 2007. Waiting time distributions for clusters of complex molecules. *EuroPhys. Lett.*: 38003.

54. Shuai, J. W., and P. Jung. 2002. Stochastic properties of Ca^{2+} release of inositol 1,4,5-trisphosphate receptor clusters. *Biophys. J.* 83:87–97.

55. Shuai, J. W., and P. Jung. 2003. Optimal ion channel clustering for intracellular calcium signaling. *Proc. Natl. Acad. Sci. USA.* 100:506–510.

56. Hinch, R. 2004. A mathematical analysis of the generation and termination of calcium sparks. *Biophys. J.* 86:1293–1307.

57. Qian, H. 2011. Nonlinear stochastic dynamics of mesoscopic homogeneous biochemical reaction systems—an analytical theory. *Nonlinearity.* 24:R19–R49.

58. Rovetti, R., K. K. Das, …, Y. Shiferaw. 2007. Macroscopic consequences of calcium signaling in microdomains: a first-passage-time approach. *Phys. Rev. E Stat. Nonlin. Soft Matter Phys.* 76:051920.

59. Wieder, N., R. H. A. Fink, and F. Wegner. 2011. Exact and approximate stochastic simulation of intracellular calcium dynamics. *J. Biomed. Biotechnol.* 2011:572492.

60. Wegner, F., N. Wieder, and R. H. A. Fink. 2012. Simulation Strategies for Calcium Microdomains and Calcium-Regulated Calcium Channels. Springer, Dordrecht, The Netherlands, pp. 553–567.

61. Fox, R. F., and Y. Lu. 1994. Emergent collective behavior in large numbers of globally coupled independently stochastic ion channels. *Phys. Rev. E Stat. Phys. Plasmas Fluids Relat. Interdiscip. Topics.* 49:3421–3431.

62. White, J. A., J. T. Rubinstein, and A. R. Kay. 2000. Channel noise in neurons. *Trends Neurosci.* 23:131–137.

63. Kepler, T. B., and T. C. Elston. 2001. Stochasticity in transcriptional regulation: origins, consequences, and mathematical representations. *Biophys. J.* 81:3116–3136.

64. Chow, C. C., and J. A. White. 1996. Spontaneous action potentials due to channel fluctuations. *Biophys. J.* 71:3013–3021.

65. Tao, Y., Y. Jia, and T. G. Dewey. 2005. Stochastic fluctuations in gene expression far from equilibrium: ω expansion and linear noise approximation. *J. Chem. Phys.* 122:124108.

66. Grima, R. 2009. Investigating the robustness of the classical enzyme kinetic equations in small intracellular compartments. *BMC Syst. Biol.* 3:101.

67. Thomas, P., H. Matuschek, and R. Grima. 2012. Computation of biochemical pathway fluctuations beyond the linear noise approximation using $_i$NA. *In* 2012 IEEE International Conference on Bioinformatics and Biomedicine (BIBM). IEEE, Piscataway, NJ. 1–5.

68. Pahle, J., J. D. Challenger, …, A. J. McKane. 2012. Biochemical fluctuations, optimization and the linear noise approximation. *BMC Syst. Biol.* 6:86.

69. Bers, D. M. 2002. Cardiac excitation-contraction coupling. *Nature.* 415:198–205.

70. Rutter, G. A., T. Tsuboi, and M. A. Ravier. 2006. Ca^{2+} microdomains and the control of insulin secretion. *Cell Calcium.* 40:539–551.

71. Villalobos, C., L. Núñez, …, J. García-Sancho. 2001. Mitochondrial $[Ca^{2+}]$ oscillations driven by local high $[Ca^{2+}]$ domains generated by spontaneous electric activity. *J. Biol. Chem.* 276:40293–40297.

72. Pethig, R., M. Kuhn, …, L. F. Jaffe. 1989. On the dissociation constants of BAPTA-type calcium buffers. *Cell Calcium.* 10:491–498.